Convective Asymmetries Measured by XDD Dropsondes in Tropical Cyclones

***T. Connor Nelson and Lee Harrison**

Atmospheric Sciences Research Center

University at Albany, SUNY

18 October 2016

2016 TCI Workshop

Goals of Analysis

- Examine the convective updrafts and downdrafts (UDs)
  - Marty (27 – 28 October), Joaquin (2 – 5 October), and Patricia (20 – 23 October)
- Derive vertical velocity using dropsonde fall speed and density correction
- Evaluate the spatial distribution of abnormally strong UDs ($\geq \pm 5$ m s^{-1})

Goals of Analysis

- Examine the convective updrafts and downdrafts (UDs)
  - Marty (27 – 28 October), Joaquin (2 – 5 October), and Patricia (20 – 23 October)
- Derive vertical velocity using dropsonde fall speed and density correction
- Evaluate the spatial distribution of abnormally strong UDs ($\geq \pm 5$ m s^{-1})

Goals of Analysis

- Examine the convective updrafts and downdrafts (UDs)
  - Marty (27 – 28 October), Joaquin (2 – 5 October), and Patricia (20 – 23 October)
- Derive vertical velocity using dropsonde fall speed and density correction
- Evaluate the spatial distribution of abnormally strong UDs ($\geq \pm 5$ m s^{-1})

Methodology

- Compute vertical velocity following similar to Hock and Franklin (1999); however, we use the near surface fall speed instead of drag coefficients:

$$w = V - V_f \qquad (1)$$

$$V = (F_o^2) * \sqrt{\frac{\rho_o}{\rho}} \qquad (2)$$

$$\rho = \frac{p}{(R_d * T_v)} \qquad (3)$$

- Sonde derived vertical velocities were then filtered using a nine-point binomial filter
- Evaluated based upon thresholds of moderate (≥ ± 5 m s^{-1}), strong (≥ ± 8 m s^{-1}), and extreme (≥ ± 10 m s^{-1})

Methodology

- Compute vertical velocity following similar to Hock and Franklin (1999); however, we use the near surface fall speed instead of drag coefficients:

$$w = V - V_f \qquad (1)$$

$$V = (F_o^2) * \sqrt{\frac{\rho_o}{\rho}} \qquad (2)$$

$$\rho = \frac{p}{(R_d * T_v)} \qquad (3)$$

- Sonde derived vertical velocities were then filtered using a nine-point binomial filter
- Evaluated based upon thresholds of moderate (≥ ± 5 m s^{-1}), strong (≥ ± 8 m s^{-1}), and extreme (≥ ± 10 m s^{-1})

Methodology

- Compute vertical velocity following similar to Hock and Franklin (1999); however, we use the near surface fall speed instead of drag coefficients:

$$w = V - V_f \qquad (1)$$

$$V = (F_o^2) * \sqrt{\frac{\rho_o}{\rho}} \qquad (2)$$

$$\rho = \frac{p}{(R_d * T_v)} \qquad (3)$$

- Sonde derived vertical velocities were then filtered using a nine-point binomial filter
- Evaluated based upon thresholds of moderate (≥ ± 5 m s^{-1}), strong (≥ ± 8 m s^{-1}), and extreme (≥ ± 10 m s^{-1})

Methodology

- A propensity parameter was calculated

$$\gamma = \frac{n_o}{\frac{H}{F_o} * N} \qquad (4)$$

- The environmental shear, TC intensity, and TC heading were obtained from the Statistical Hurricane Intensity Prediction Scheme (SHIPS) dataset (DeMaria and Kaplan 1994)
- The TC center was derived using a zero wind center correction to the Automated Tropical Cyclone Forecast (AFTC) Best-Track dataset from the National Hurricane Center (NHC)
  - Similar to Creasey and Elsberry (2016)
- Radius of maximum wind (RMW) was obtained by examining the top 99.8 percentile of tangential wind speeds
  - Take the mean distance to the TC center of this data
  - Evaluate data points relative to the RMW normalized radius (R*)

Methodology

- A propensity parameter was calculated

$$\gamma = \frac{n_o}{\frac{H}{F_o} * N} \qquad (4)$$

- The environmental shear, TC intensity, and TC heading were obtained from the Statistical Hurricane Intensity Prediction Scheme (SHIPS) dataset (DeMaria and Kaplan 1994)
- The TC center was derived using a zero wind center correction to the Automated Tropical Cyclone Forecast (AFTC) Best-Track dataset from the National Hurricane Center (NHC)
  - Similar to Creasey and Elsberry (2016)
- Radius of maximum wind (RMW) was obtained by examining the top 99.8 percentile of tangential wind speeds
  - Take the mean distance to the TC center of this data
  - Evaluate data points relative to the RMW normalized radius (R*)

Methodology

- A propensity parameter was calculated

$$\gamma = \frac{n_o}{\frac{H}{F_o} * N} \qquad (4)$$

- The environmental shear, TC intensity, and TC heading were obtained from the Statistical Hurricane Intensity Prediction Scheme (SHIPS) dataset (DeMaria and Kaplan 1994)
- The TC center was derived using a zero wind center correction to the Automated Tropical Cyclone Forecast (AFTC) Best-Track dataset from the National Hurricane Center (NHC)
  - Similar to Creasey and Elsberry (2016)
- Radius of maximum wind (RMW) was obtained by examining the top 99.8 percentile of tangential wind speeds
  - Take the mean distance to the TC center of this data
  - Evaluate data points relative to the RMW normalized radius (R*)

Methodology

- A propensity parameter was calculated

$$\gamma = \frac{n_o}{\frac{H}{F_o} * N} \qquad (4)$$

- The environmental shear, TC intensity, and TC heading were obtained from the Statistical Hurricane Intensity Prediction Scheme (SHIPS) dataset (DeMaria and Kaplan 1994)
- The TC center was derived using a zero wind center correction to the Automated Tropical Cyclone Forecast (AFTC) Best-Track dataset from the National Hurricane Center (NHC)
  - Similar to Creasey and Elsberry (2016)
- Radius of maximum wind (RMW) was obtained by examining the top 99.8 percentile of tangential wind speeds
  - Take the mean distance to the TC center of this data
  - Evaluate data points relative to the RMW normalized radius (R*)

Spread of Data Points

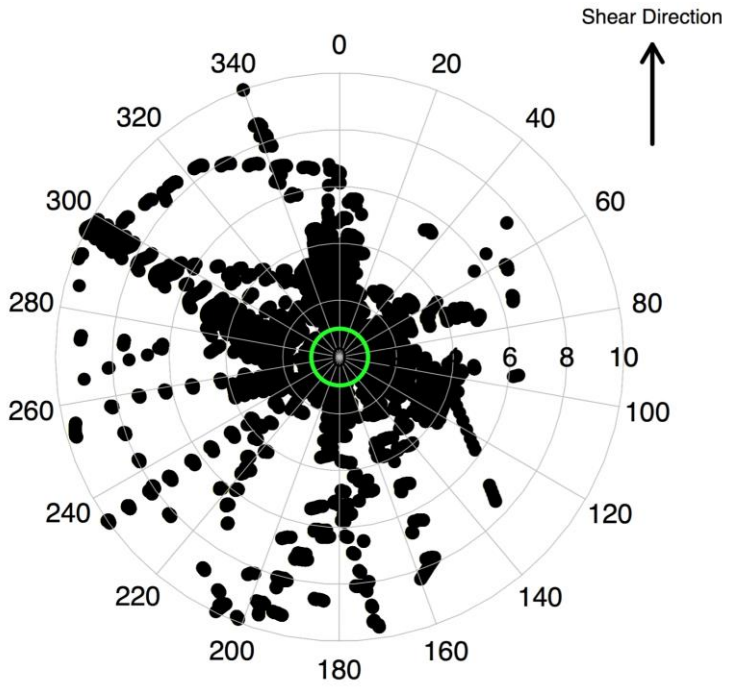

Within 10R*

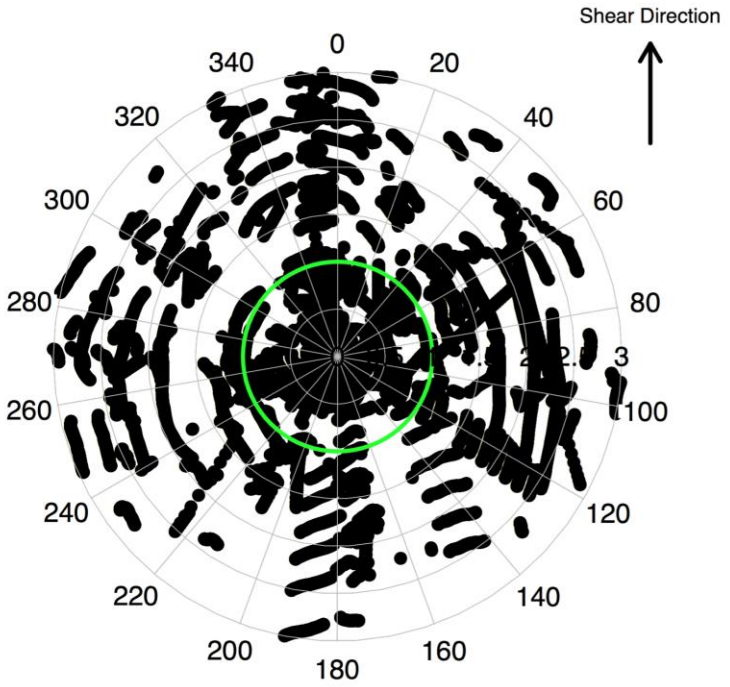

Within 3R*

- Great coverage inside R* = 10
- Outside R* = 10, preference for DSL and USL quadrants
  - Void in outer R* values in DSR

Spread of Data Points

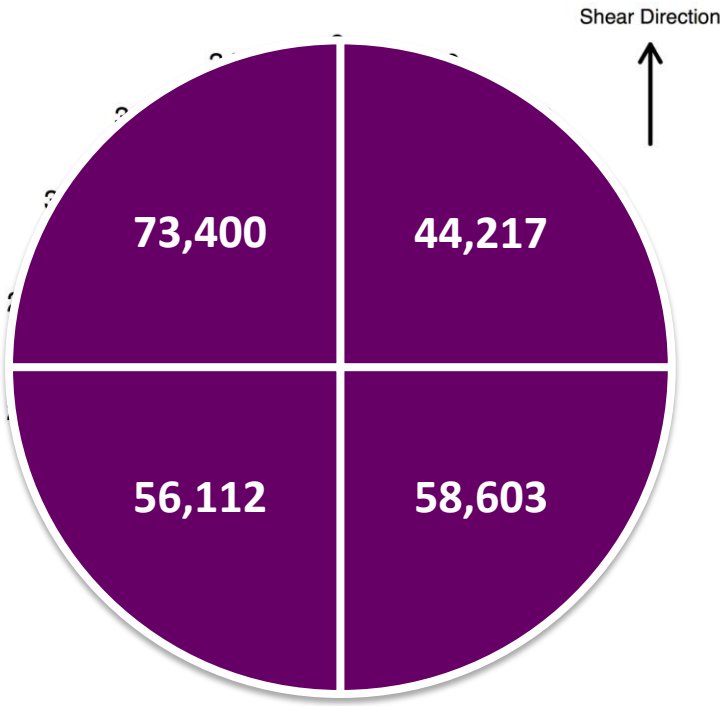

Within 10R*

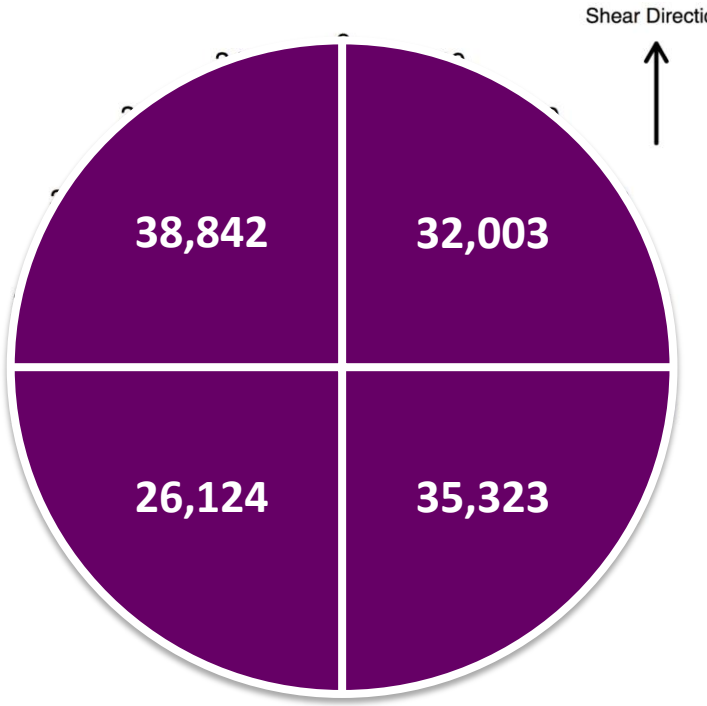

Within 3R*

- Definite radial and azimuthal sampling asymmetry
- Will have to be taken into account

Combined Data Set: CFAD

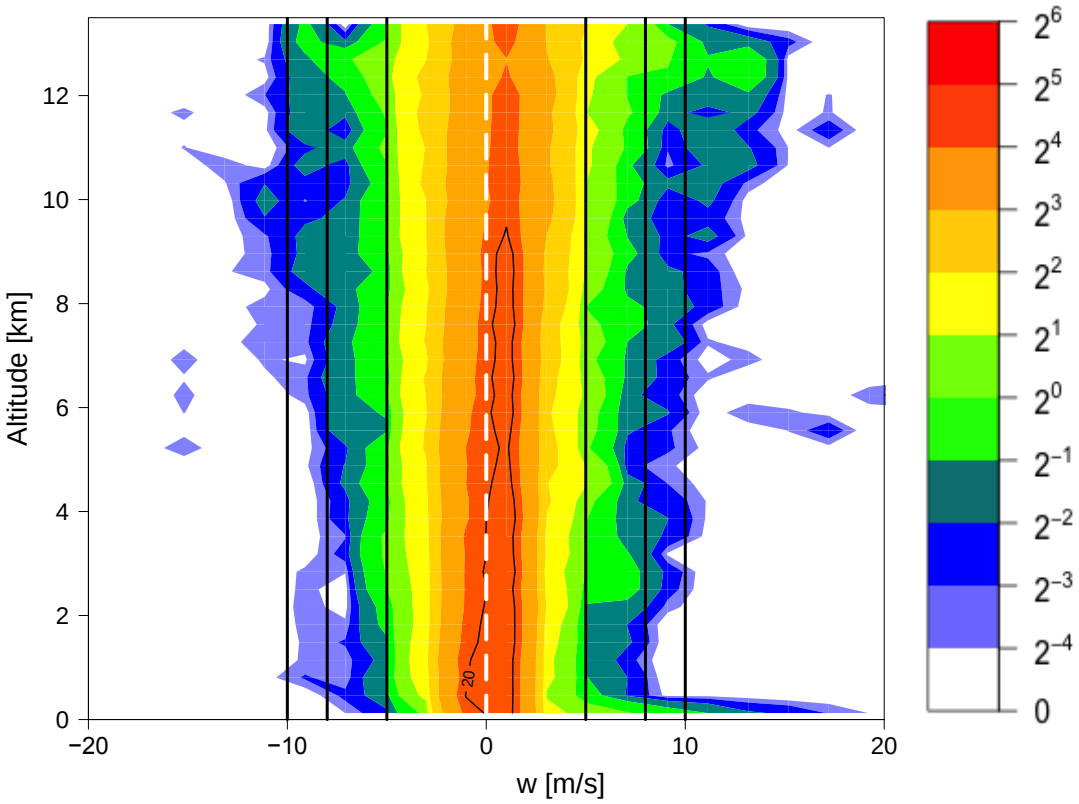

Combined Data Set: CFAD

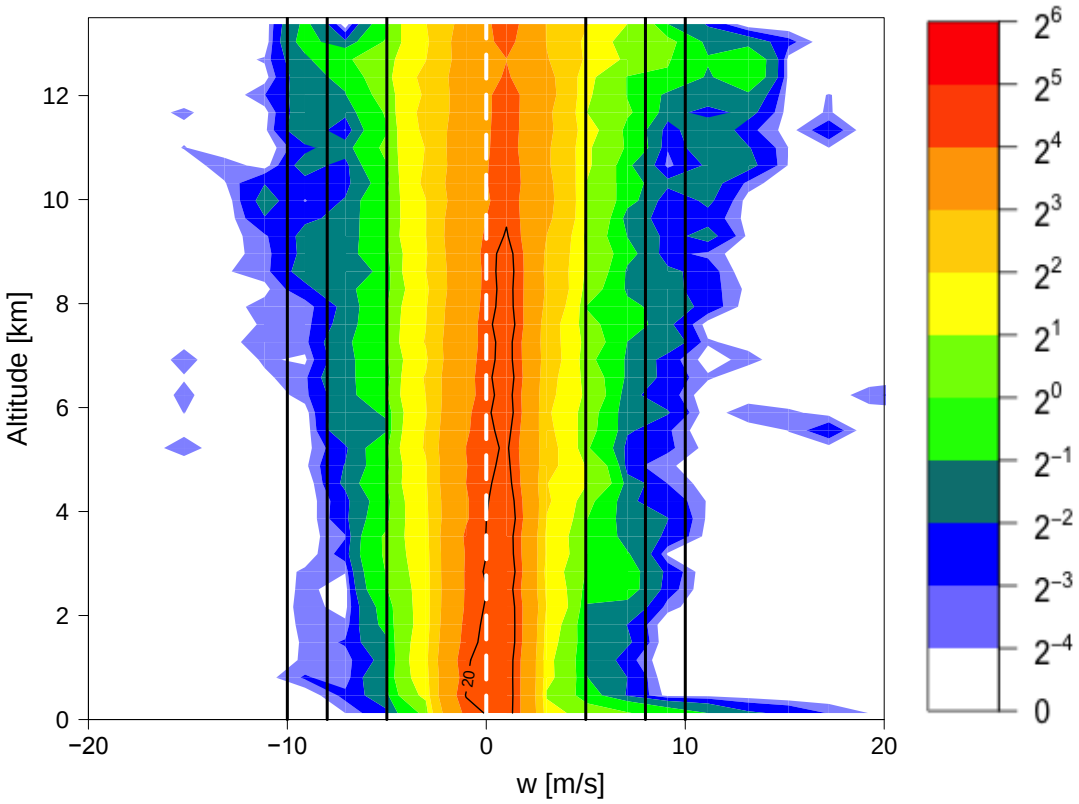

- Overall, distribution skewed towards positive values of vertical velocity
- Exhibits ‘wedge’ shape
- Downdrafts weaker than moderate strength had very little altitudinal variability
- For updrafts weaker than the moderate category, strength increased aloft

Combined Data Set: CFAD

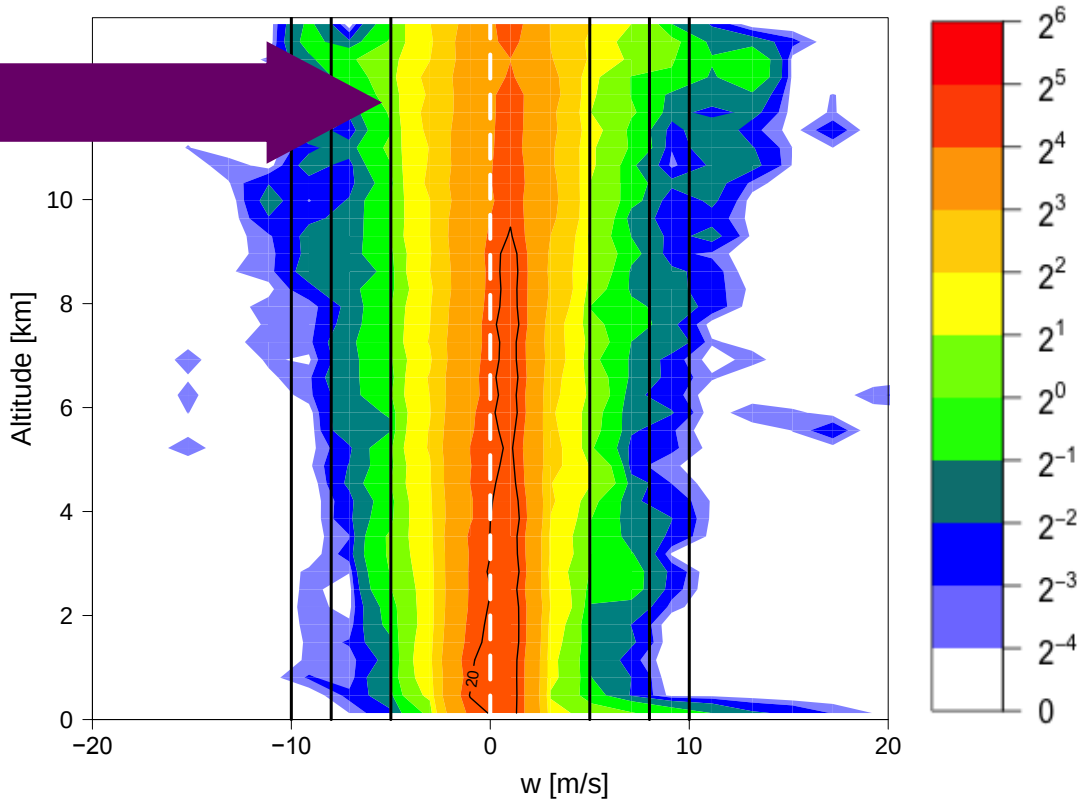

- Moderate downdrafts were trimodal with the strongest peak aloft at 12.5 km
- Secondary peaks in the midlevels (6 – 8 km) and lower levels (2 – 5 km)

Combined Data Set: CFAD

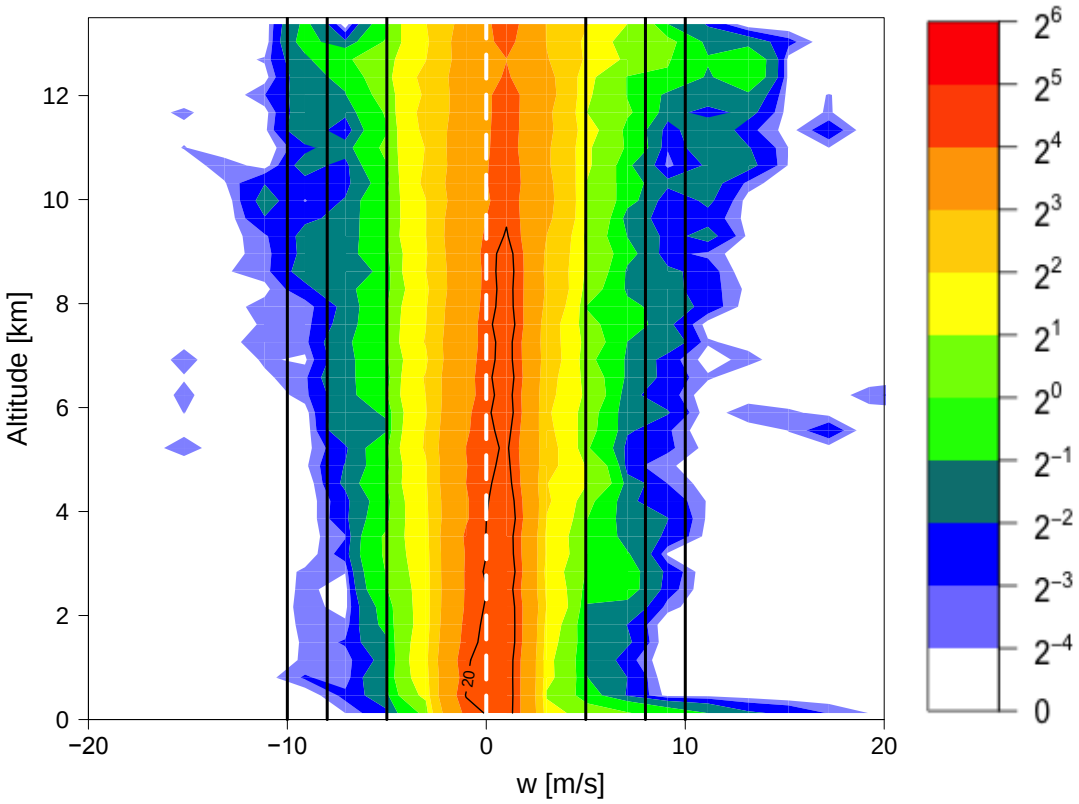

- Strong and extreme downdrafts had similar profiles
- Strong downdrafts tended to occur in mid- and upper-levels
- Extreme downdrafts occurred aloft at 12 km

Combined Data Set: CFAD

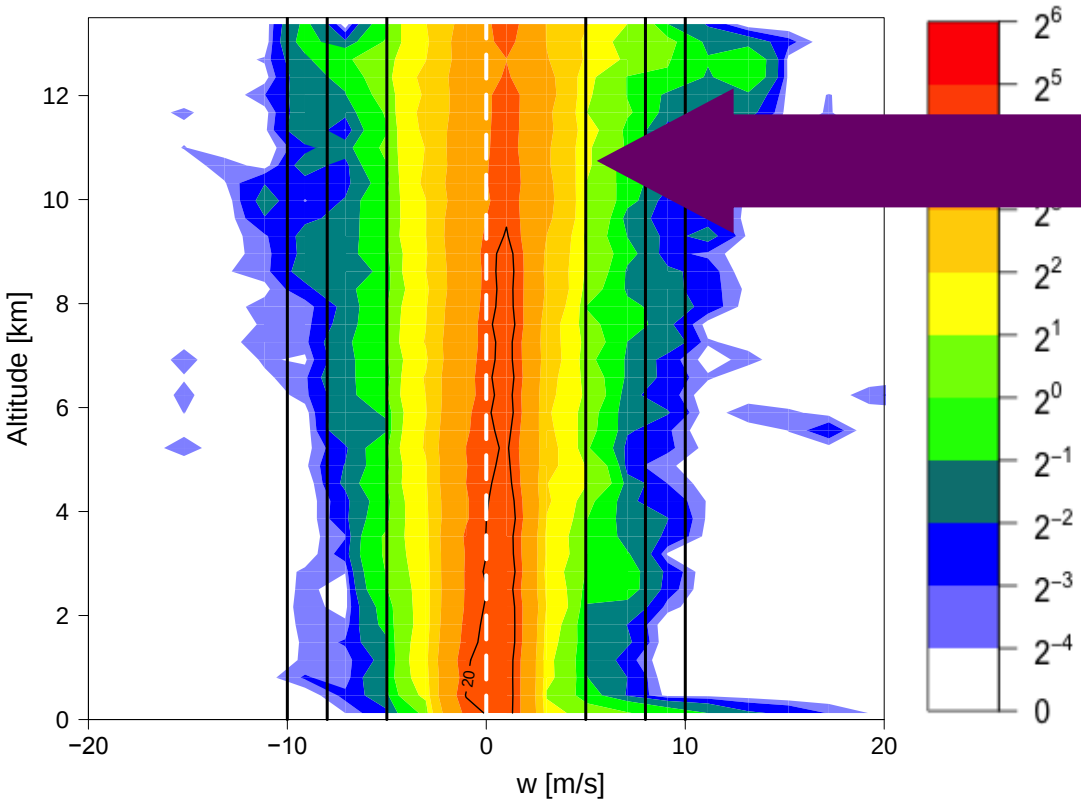

- Moderate updrafts maximized in occurrence aloft and mid-levels
- Strength increases aloft

Combined Data Set: CFAD

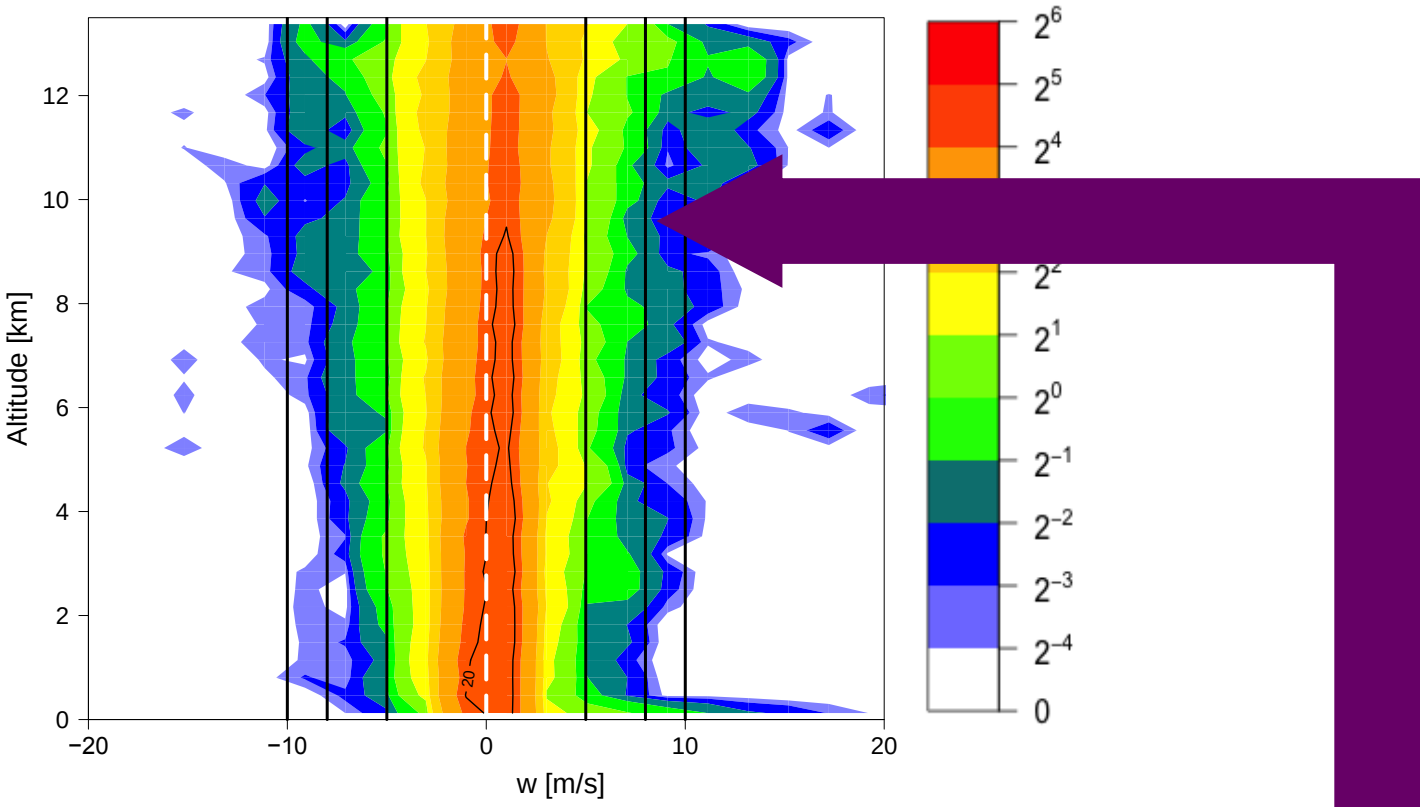

- Strong updrafts were trimodal
- Peak aloft at 12 km
- Secondary peaks at 2.5 km and 8 km

Combined Data Set: CFAD

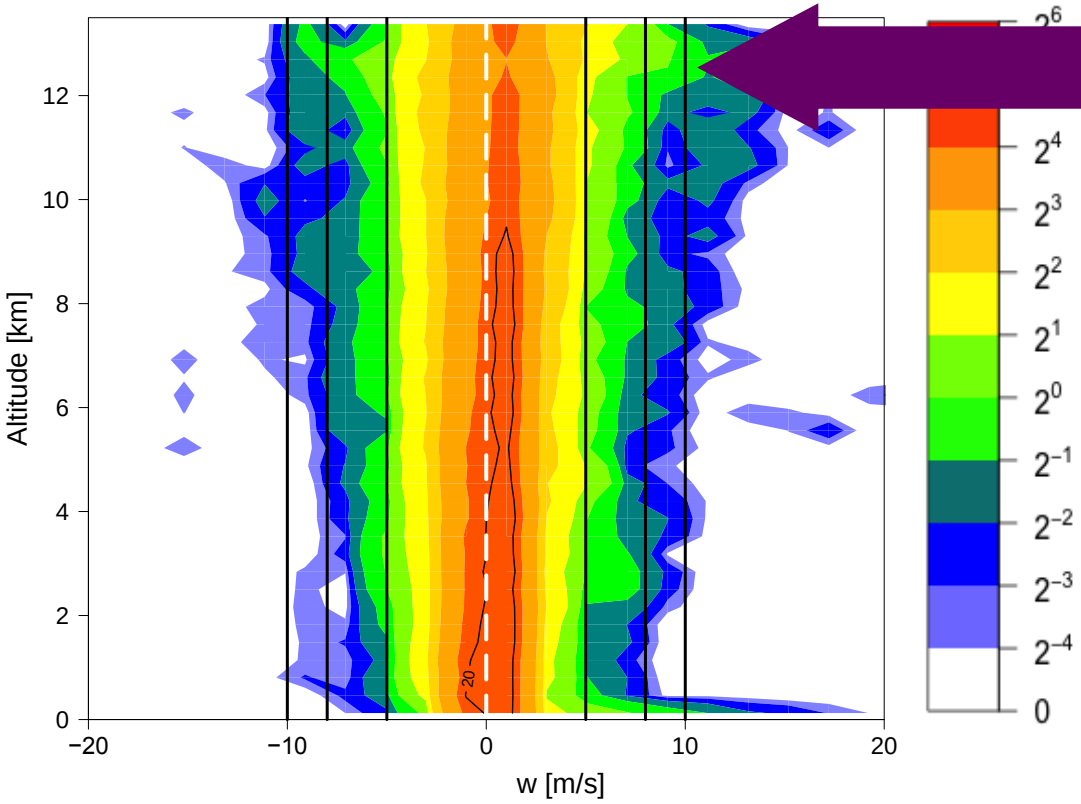

- Extreme were mainly above 8 km and maximized at 12 km

Combined Data Set: CFAD

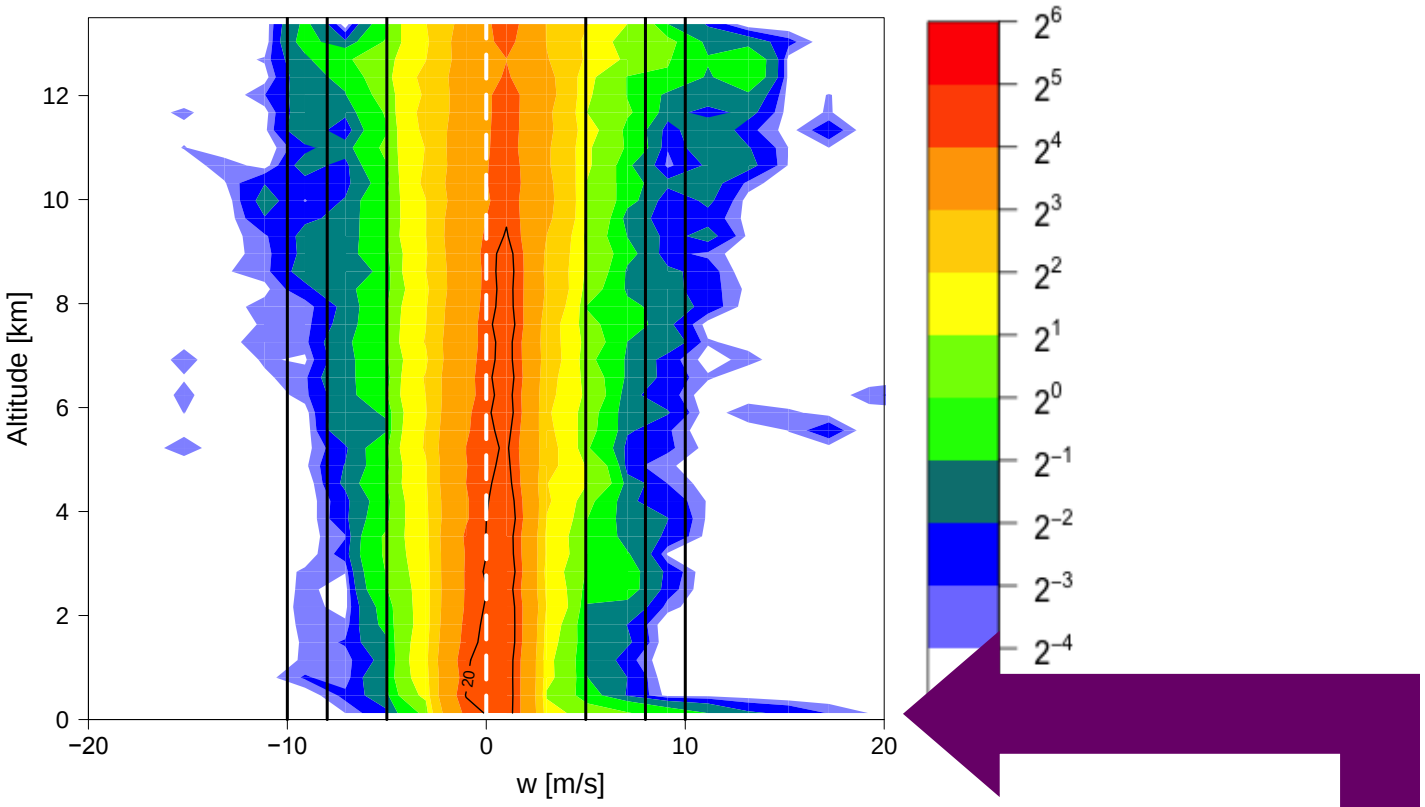

- Presence of near-surface vertical velocity maxima (Stern et al. 2016)

Combined Data Set: CFRD

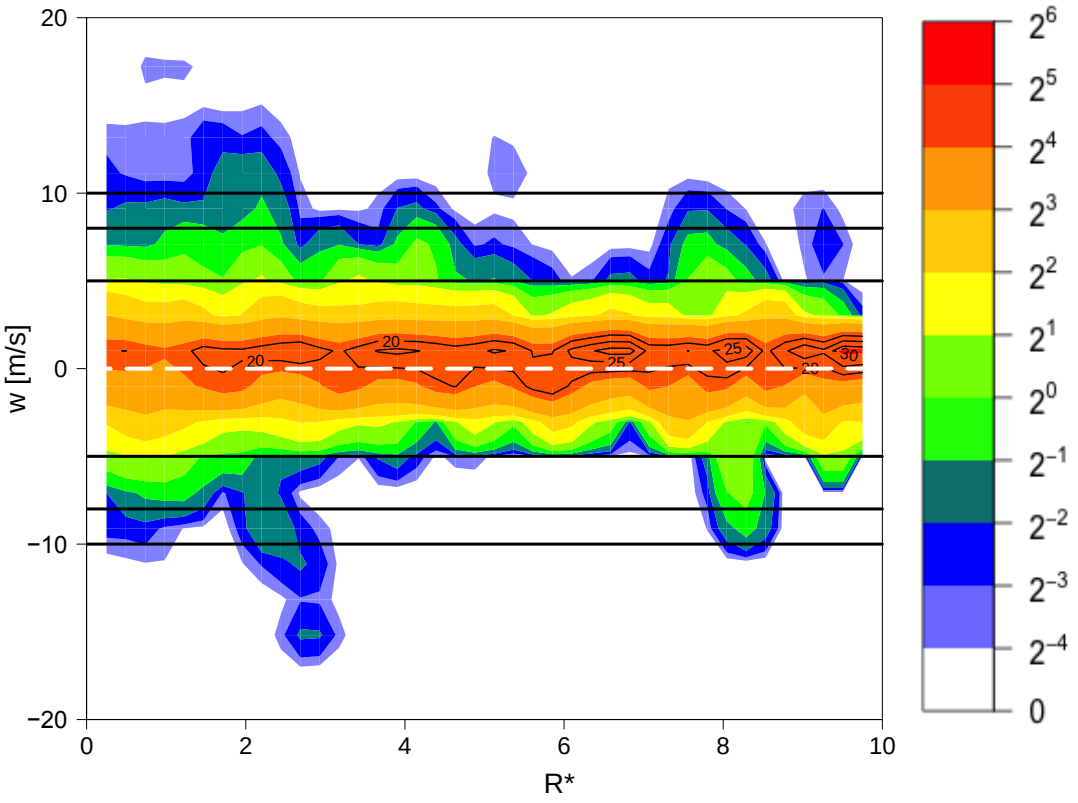

- In a general sense, there was a decrease in vertical velocity maxima with increasing radius outside of the inner core (~ 3R*)
- Significant peaks of convection just outside and at the RMW (R* = 1) and near 8R*

Combined Data Set: CFRD

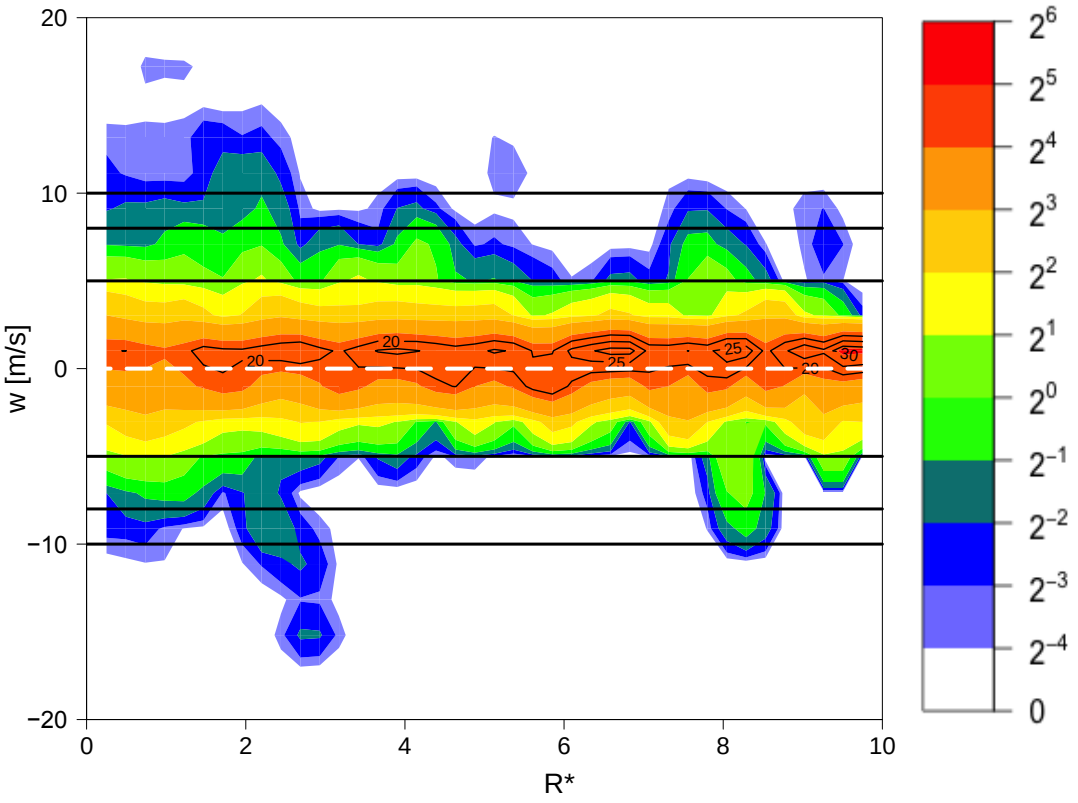

- For vertical velocities between moderate updraft to moderate downdraft, fairly constant with radius, but the frequency contours appear ‘wave-like’

Combined Data Set: CFAzD

Cyclonic Motion

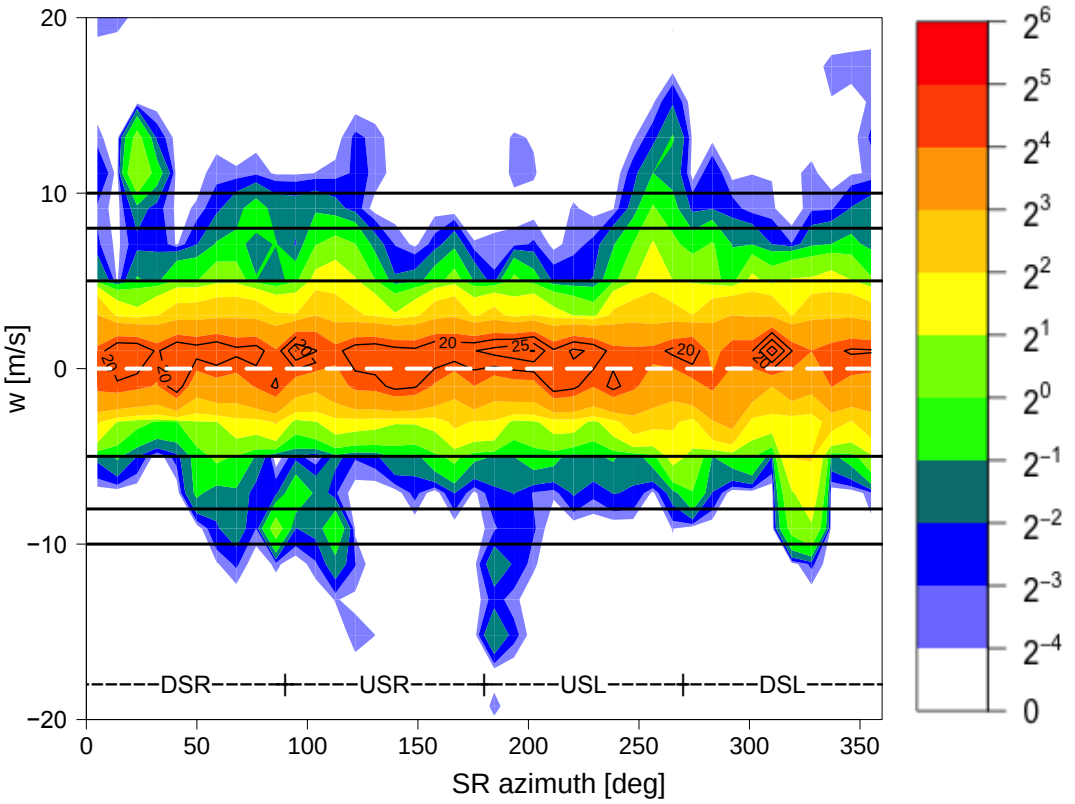

- Episodic peaks across all azimuth
- Highest percentages are above 30% with updrafts in the DSL quadrant

Combined Data Set: CFAzD

Cyclonic Motion

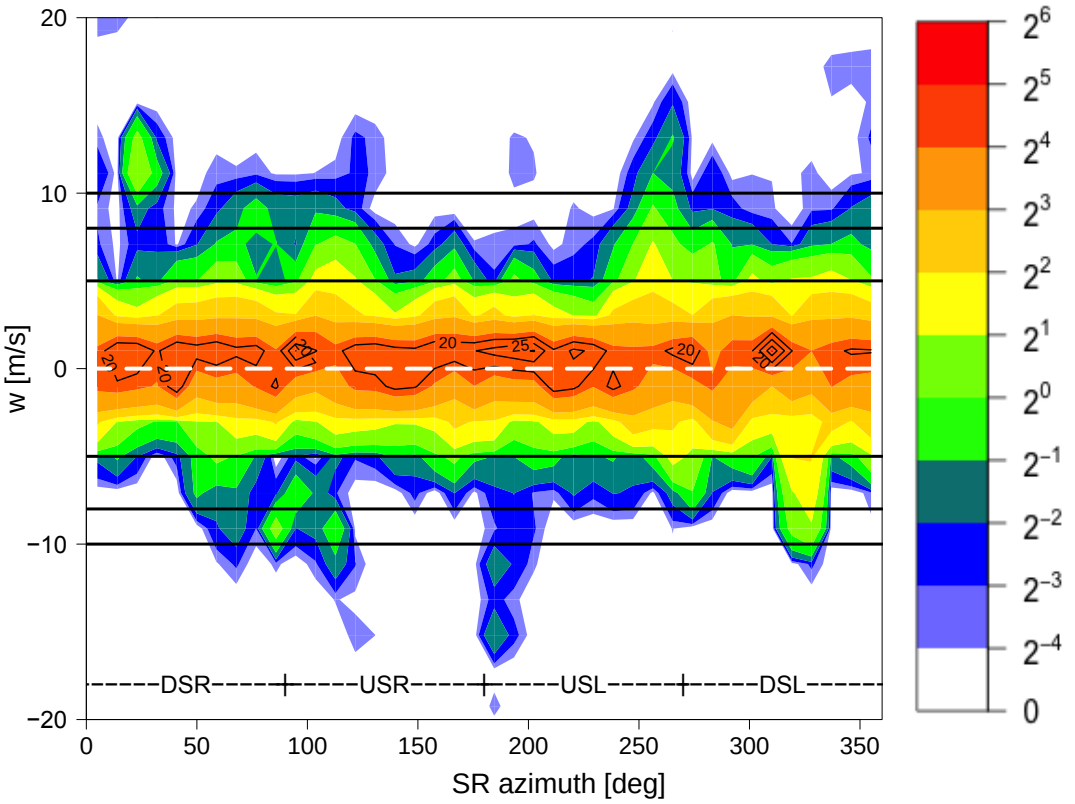

- Sharper peak of occurrence of moderate, strong, and extreme downdrafts in the DSL quadrant
- BROAD secondary increase of occurrence in the DSR quadrant and into the USR
- Odd, strong peak between the USR and USL quadrants

Combined Data Set: CFAzD

Cyclonic Motion

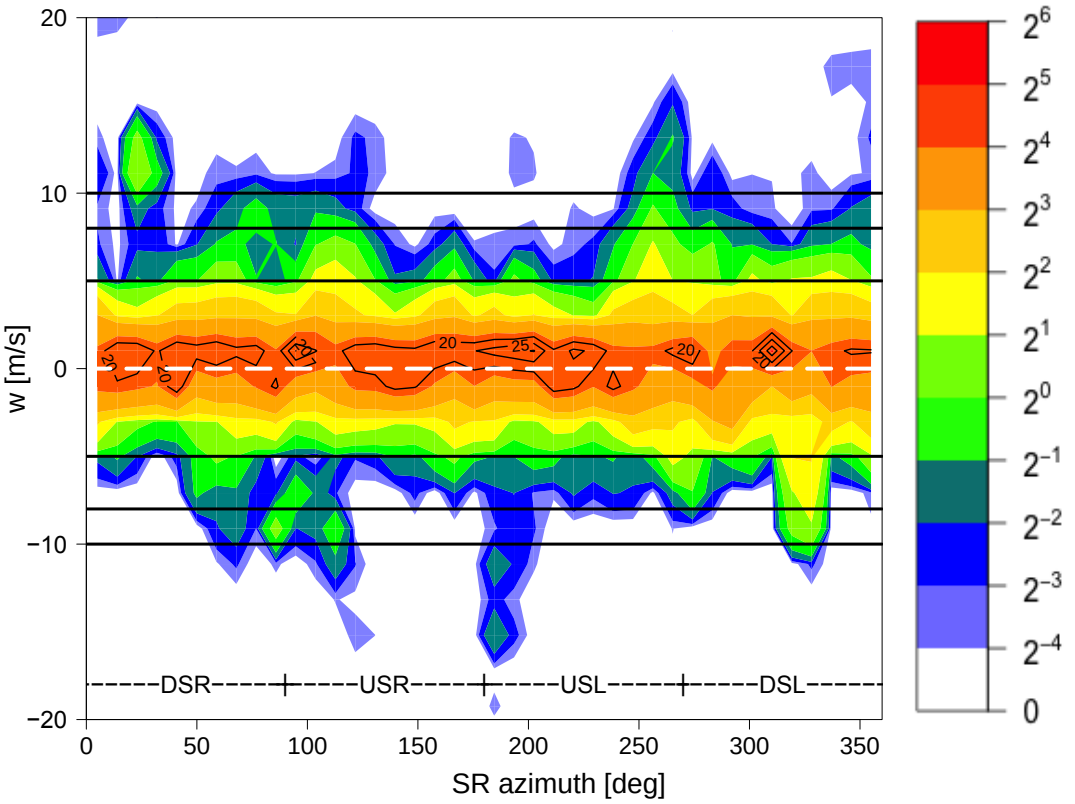

- BROAD increase of occurrence of moderate, strong, and extreme updrafts straddled the USL and DSL quadrants as well as the DSR and USR
- Strong peak near 30 – 40° in the DSR

Combined Data Set: CFAzD

Cyclonic Motion

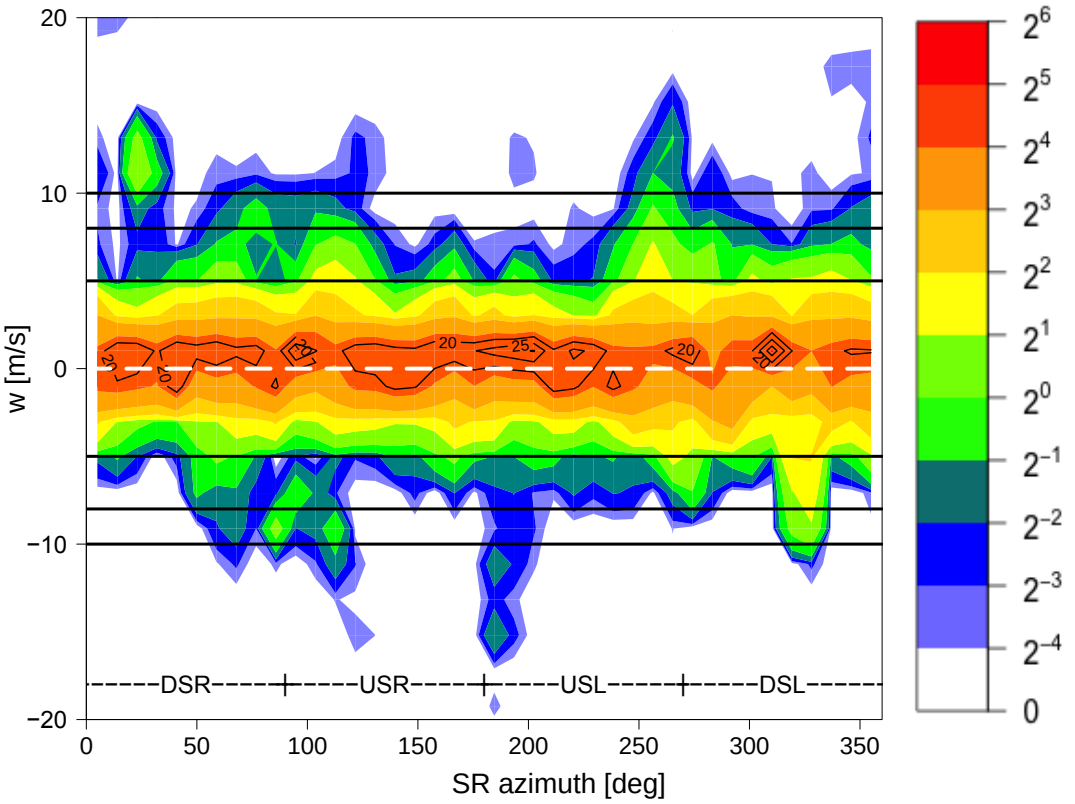

- Convectively suppressed where highest occurrences of near zero vertical velocity and shallow peaks
  - Updrafts → USR quadrant into the USL quadrant
  - Downdrafts → 0 – 50° in DSR quadrant and somewhat in USL/USR quadrants…

Gamma Values

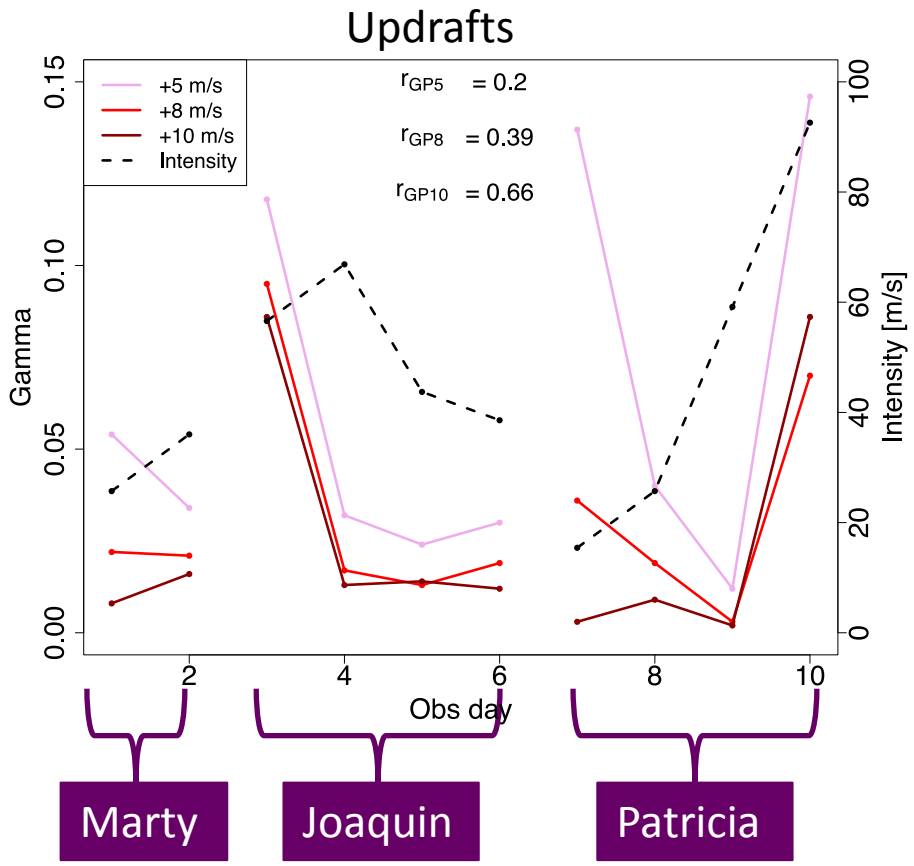

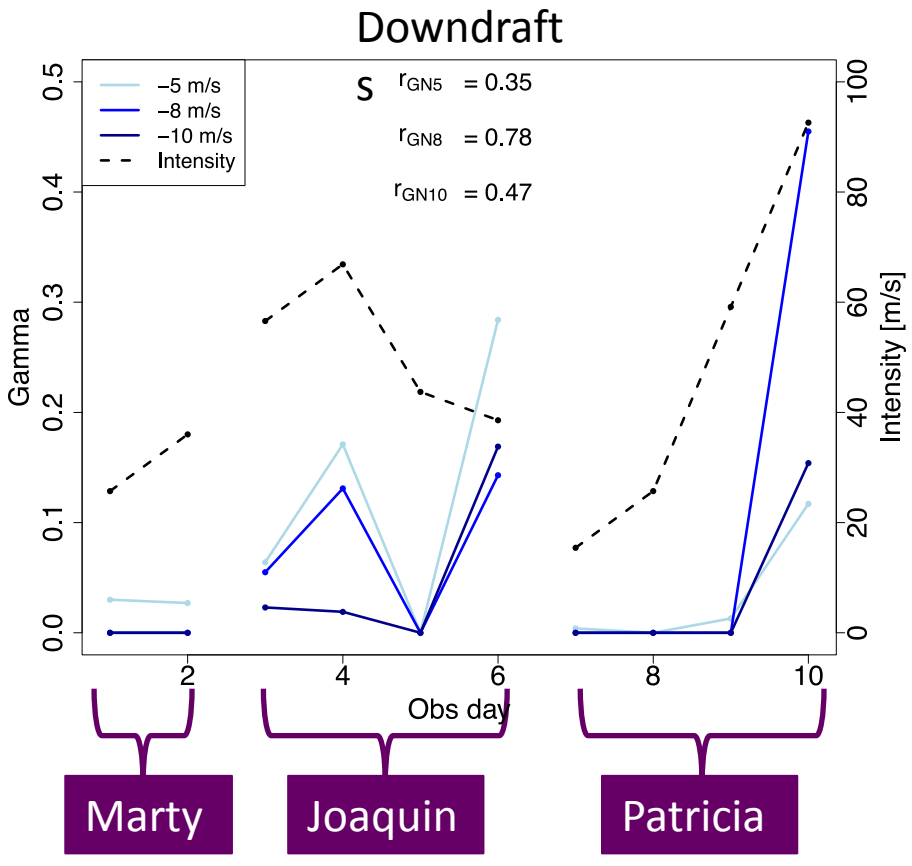

Gamma Values

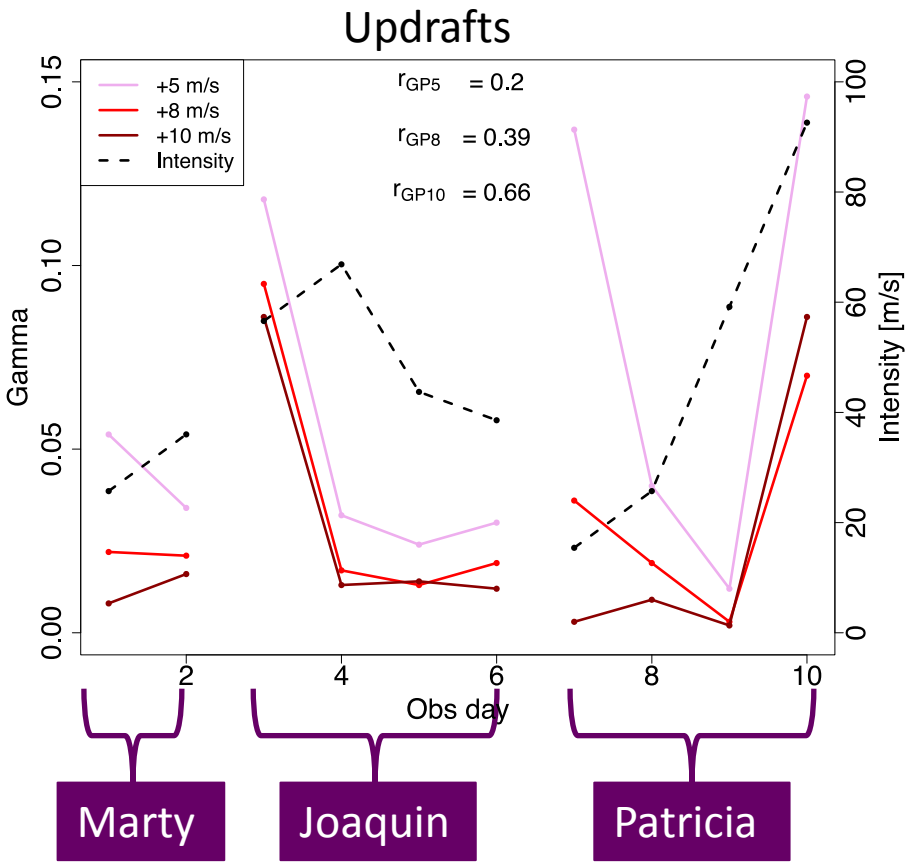

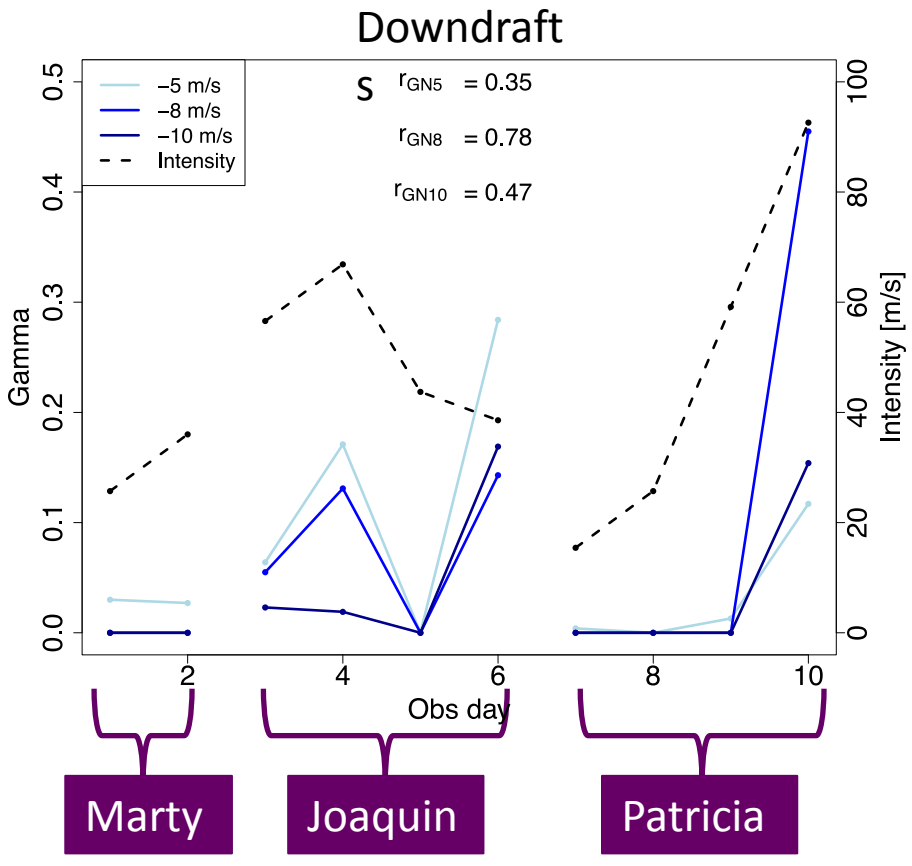

- Gamma tended to maximize for positive thresholds just before weak intensification
- Gamma tended to maximize for negative thresholds once a TC has hit its peak and begins to decay

Number of UD Data Points Inside RMW

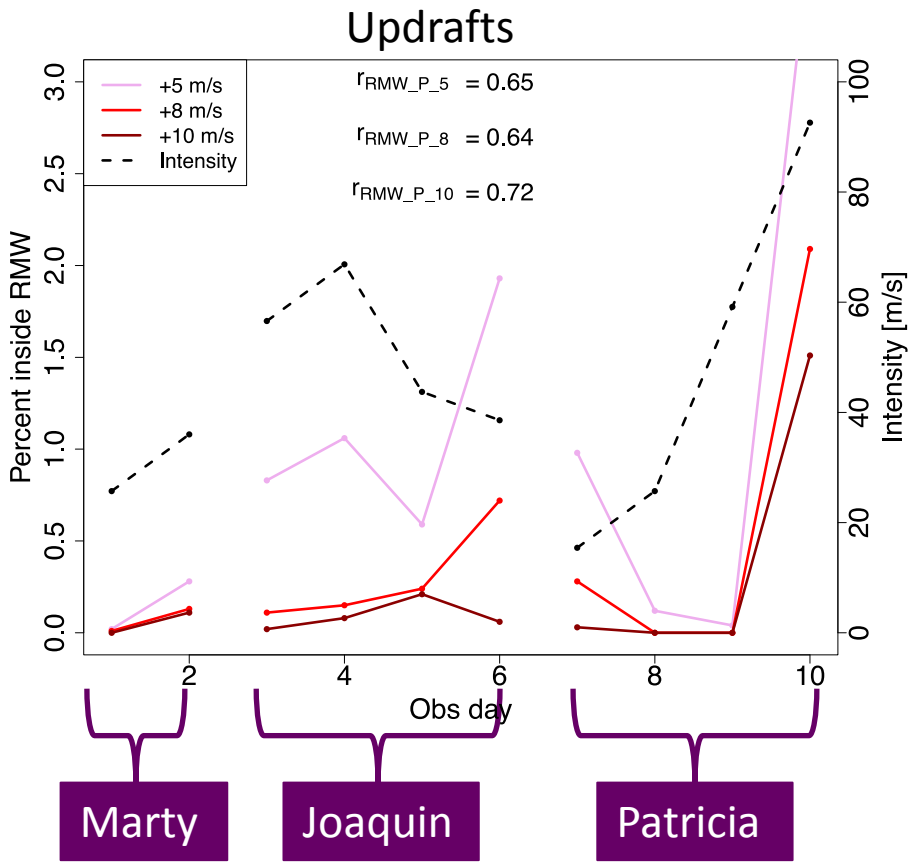

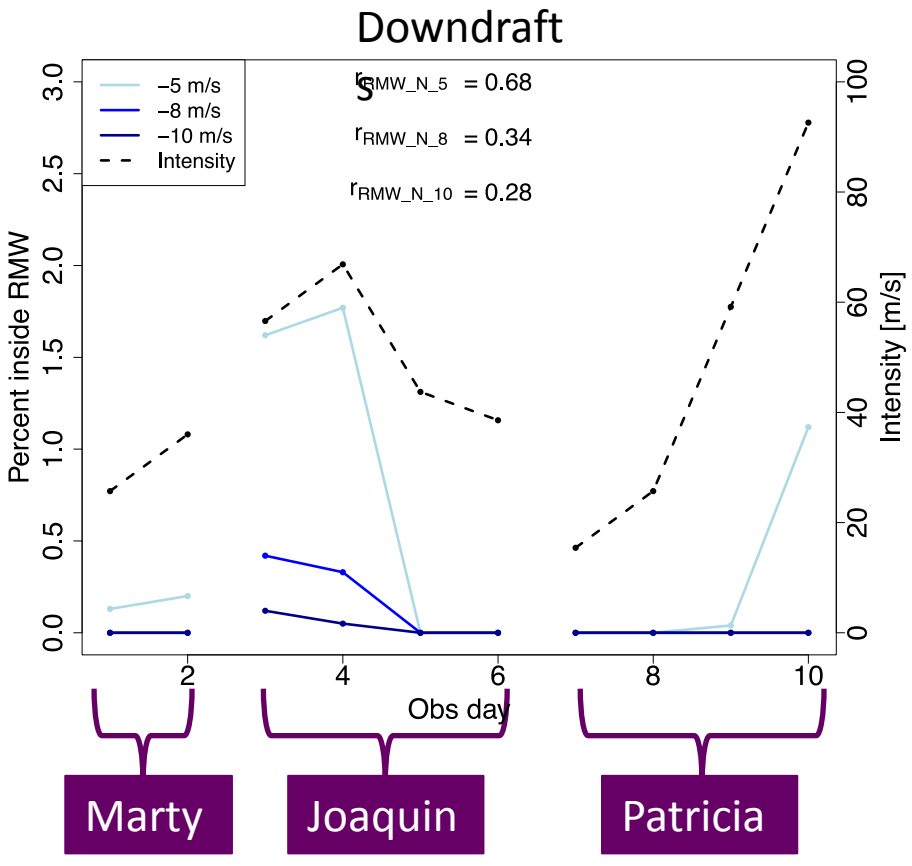

Number of UD Data Points Inside RMW

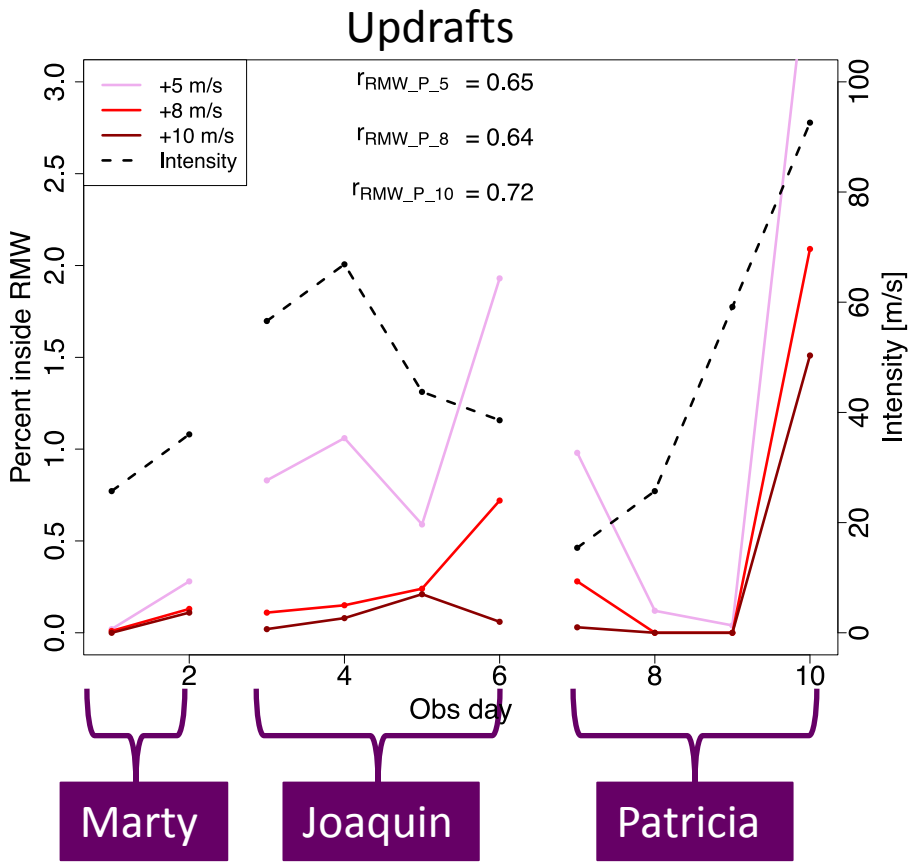

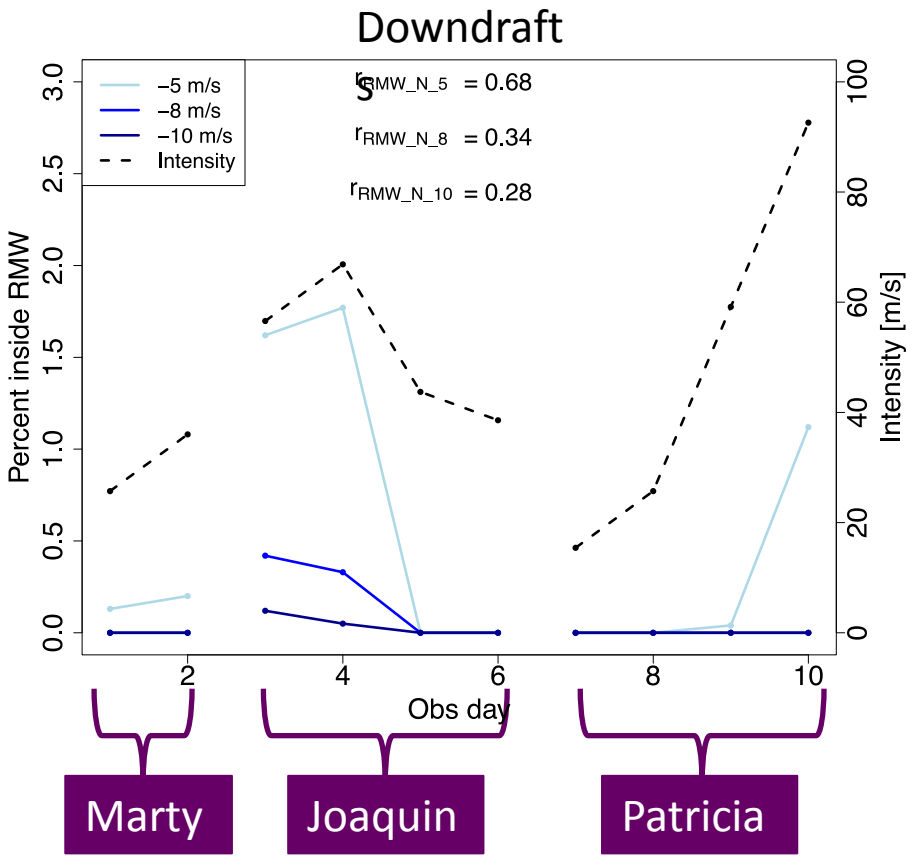

- Acceptable correlations between intensity and percent of updrafts inside the RMW for each threshold
- Percent of moderate downdrafts inside the RMW had acceptable correlation as well

Azimuthal Composite

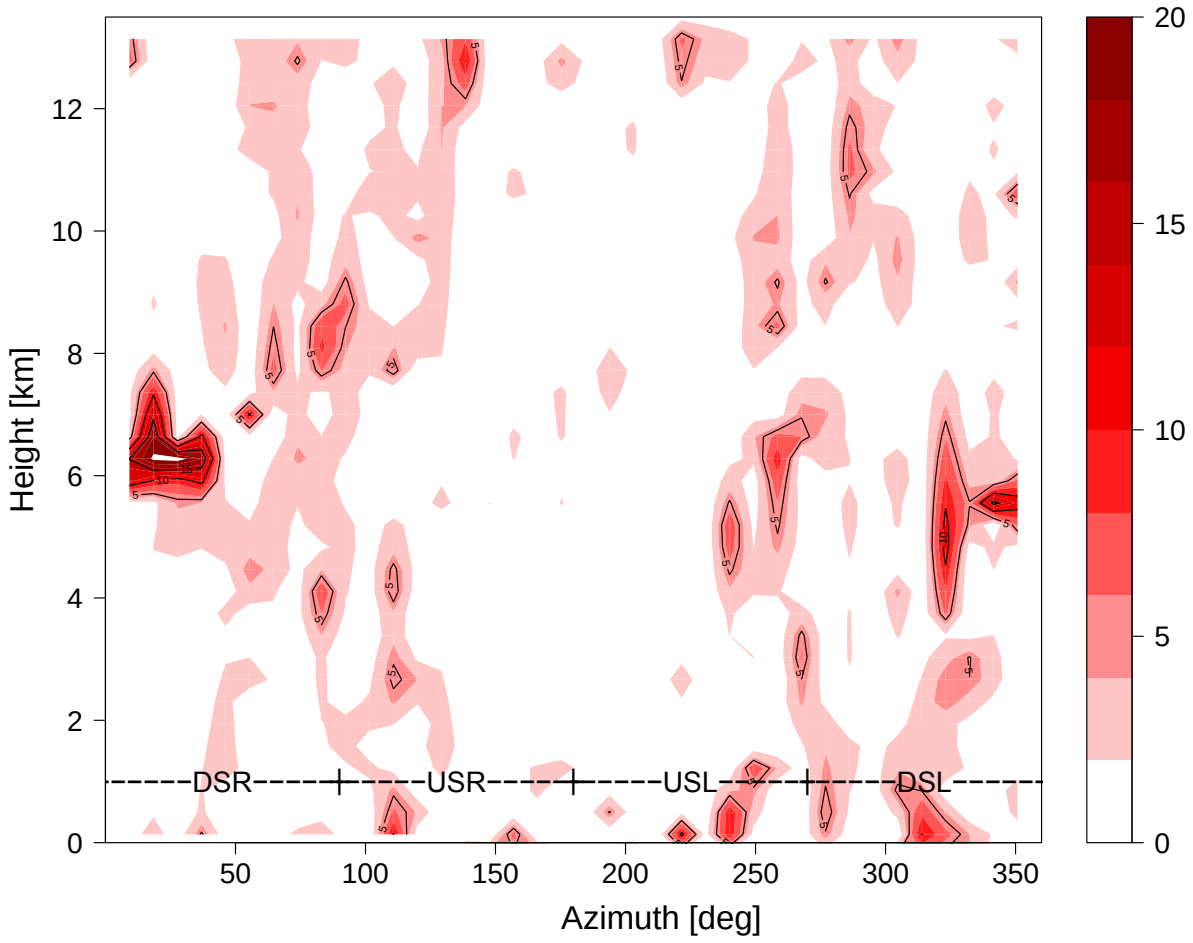

Azimuthal Composite

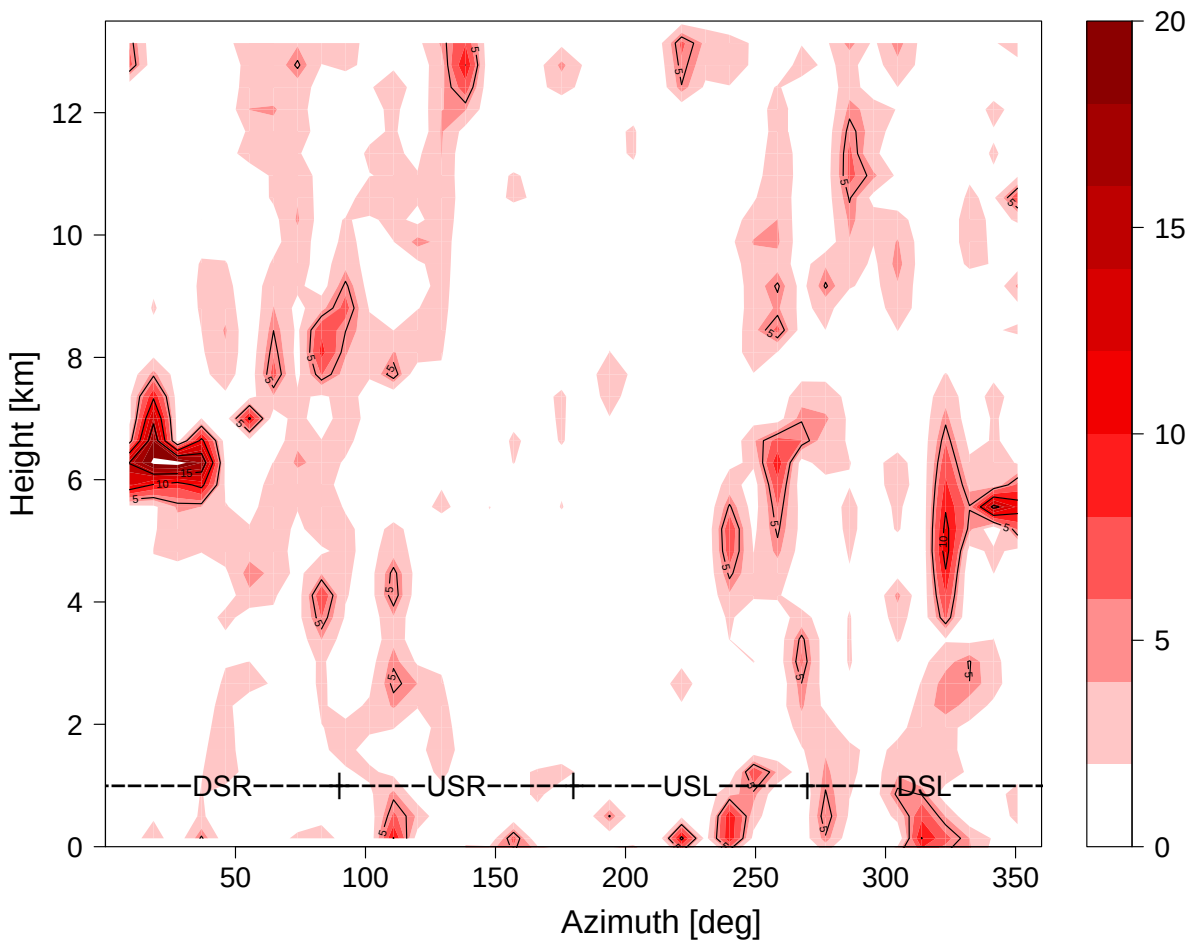

- Near surface updrafts were strongest in the DSL and USL quadrants
- Strongest updrafts occurred in the mid-levels in the DSR quadrant
- Updraft suppression between the USR and USL quadrants

Radial Composite

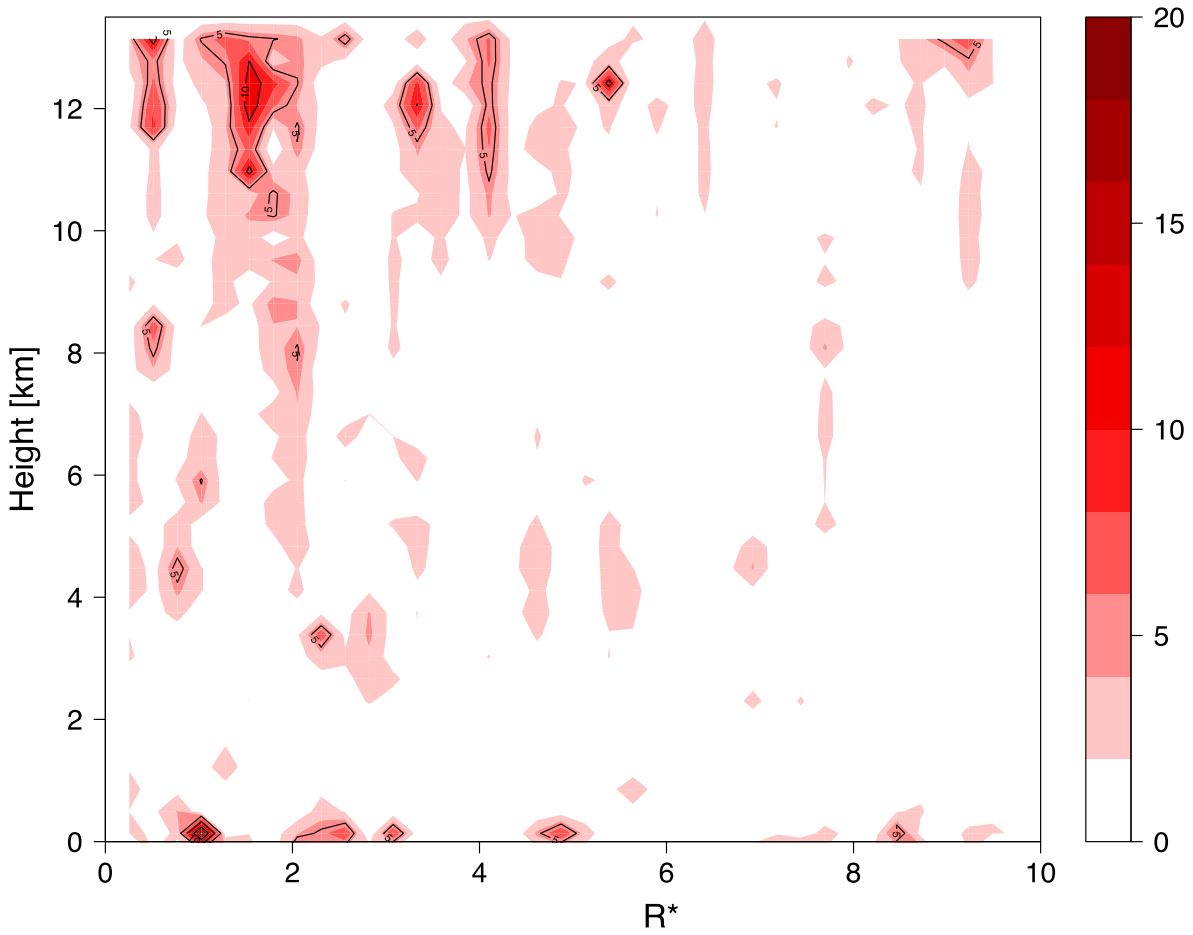

Radial Composite

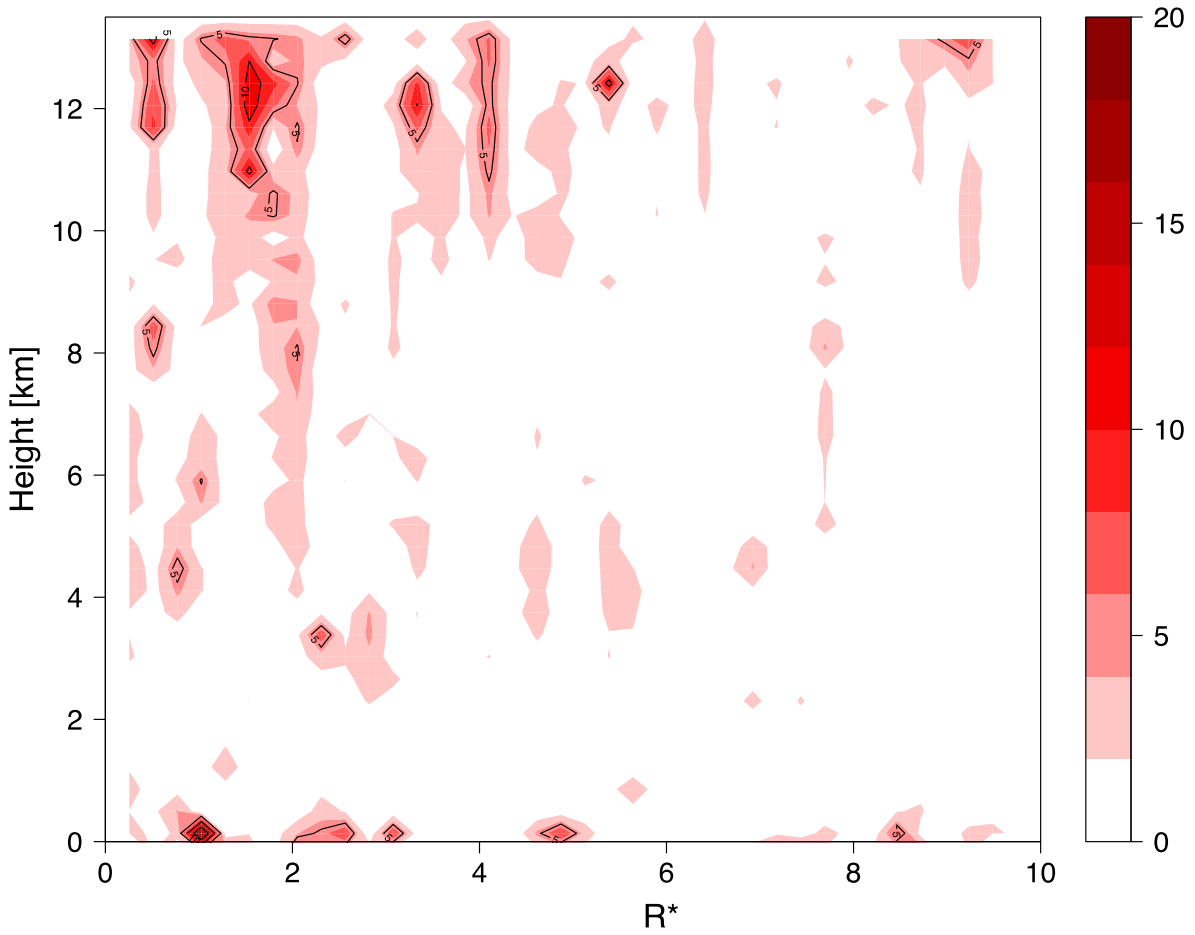

- Inner core updrafts occurred primarily aloft
- Strongest surface updrafts were in the inner core
- Weaker surface and upper level updrafts at outer radii
- Not many strong mid-level updrafts

Combining it all Together…

DSL

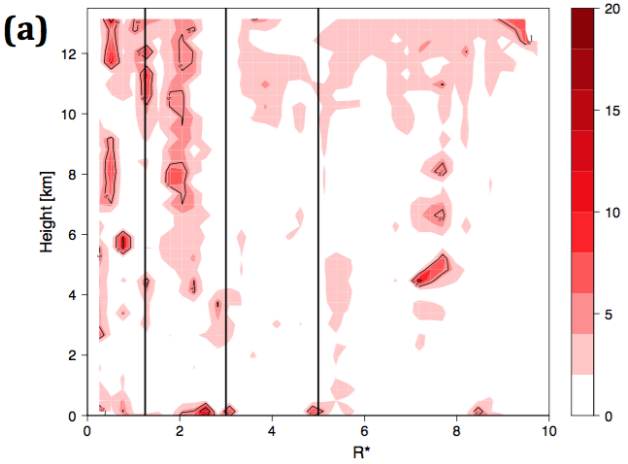

DSR

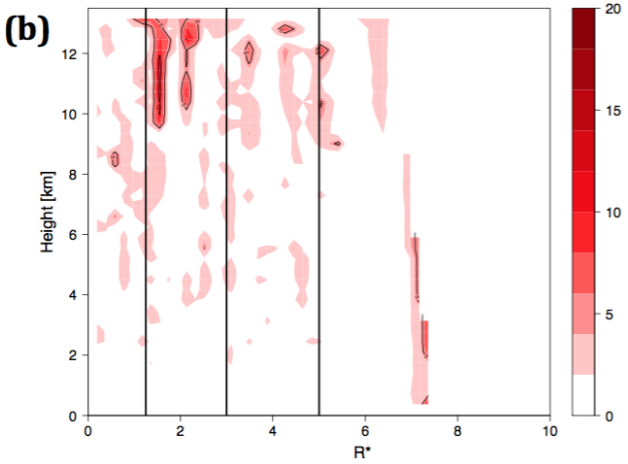

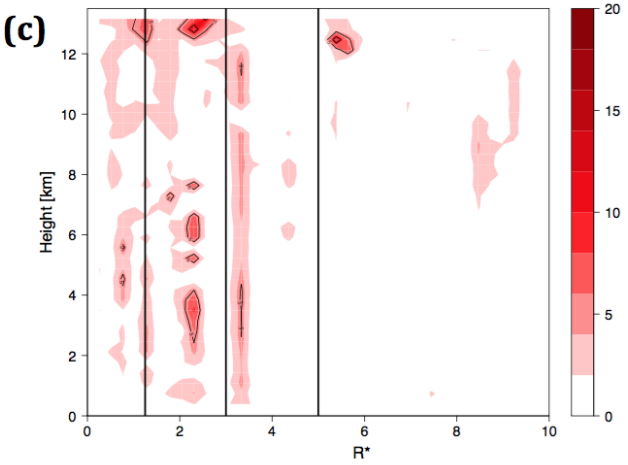

USL

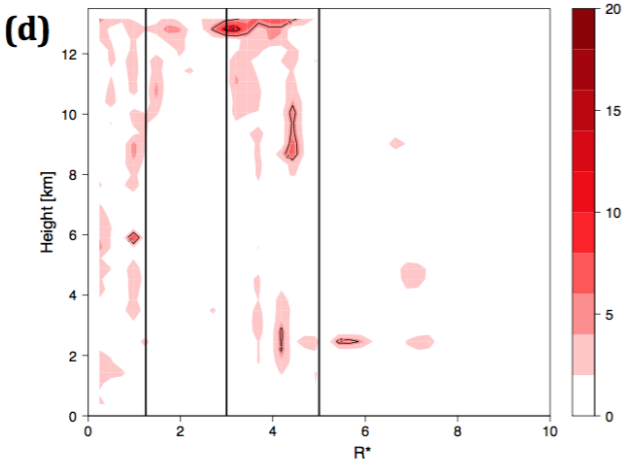

USR

Combining it all Together…

DSL

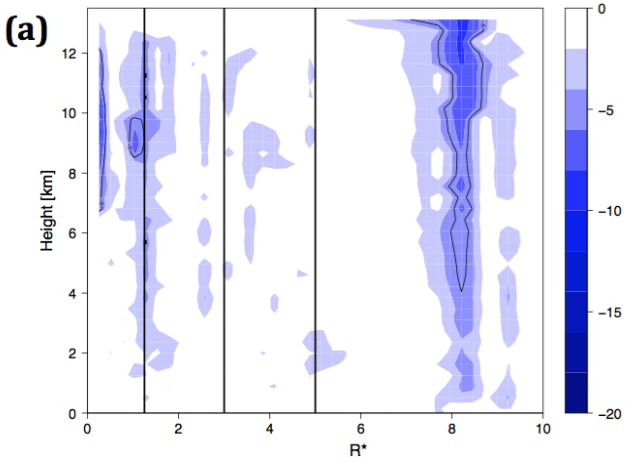

DSR

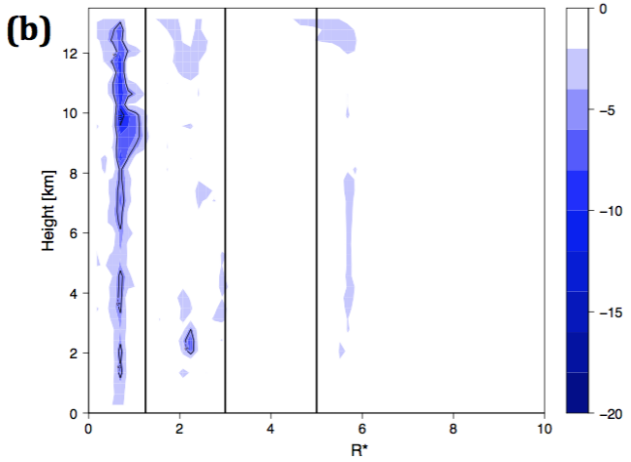

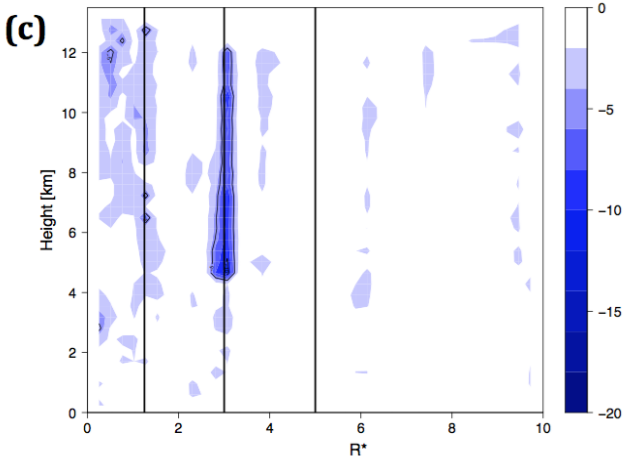

USL

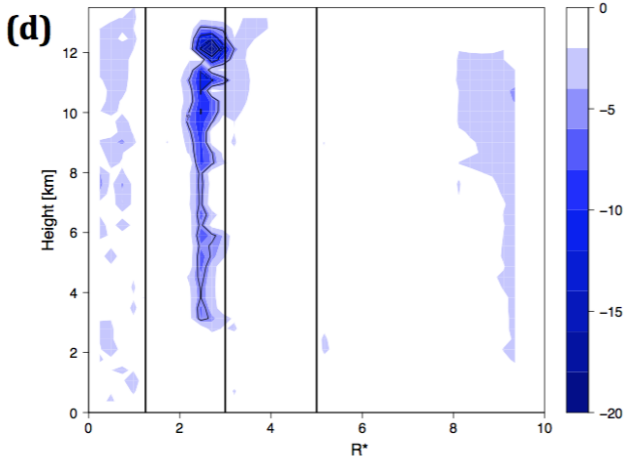

USR

Combining it all Together…

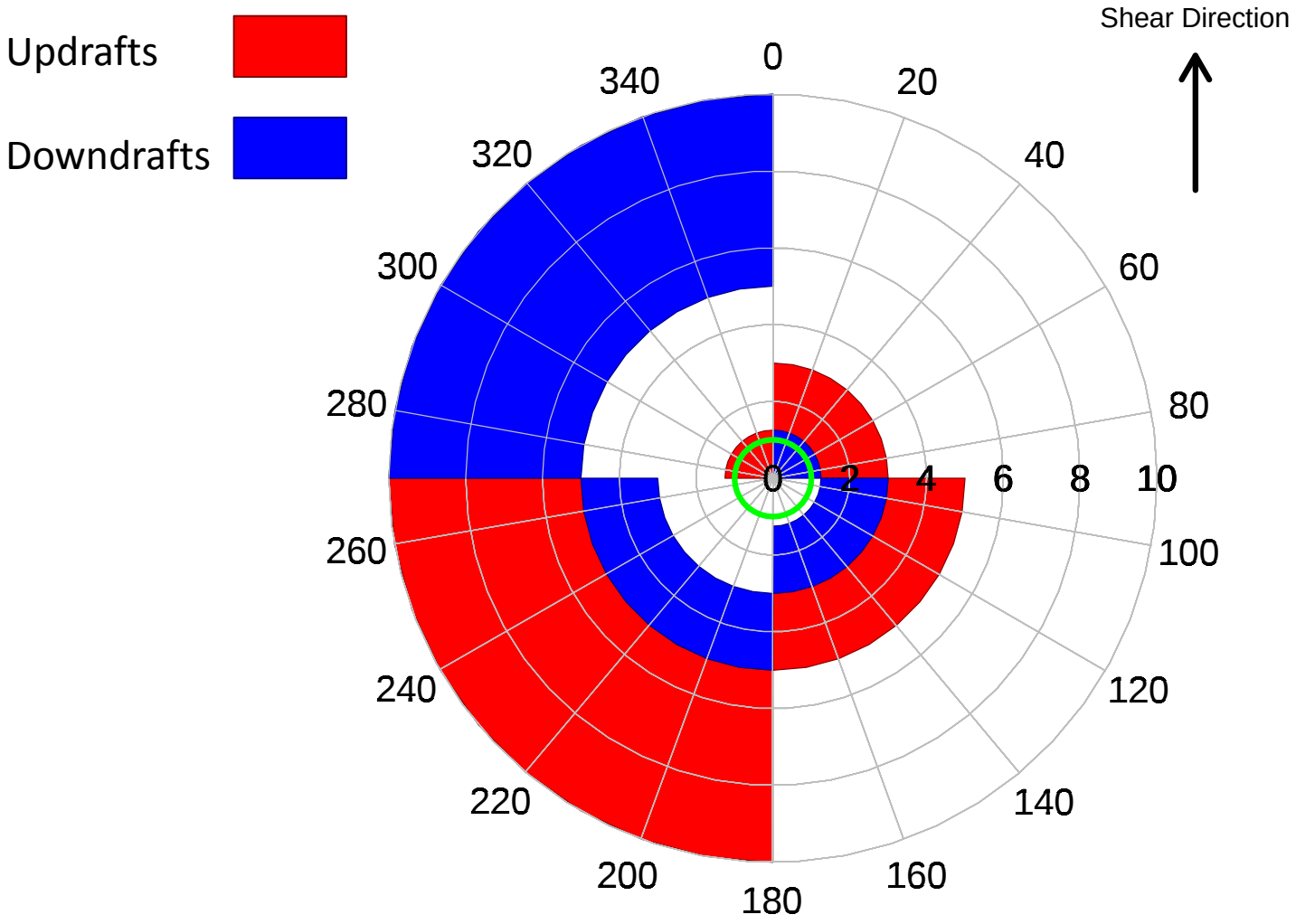

Conclusions

- Above normal convection occurred in all three TCs regardless of intensity or shear strength
- Occurred both inside and outside RMW
  - Updrafts inside RMW during peak intensities
  - Convection decreased in strength outside the inner core
- DSL updraft preference inside 1.25R*
  - Suppression in USR
- DSR downdraft preference in the inner core (1.25R* - 3R*)
- Convective strength maximized aloft
- Near-surface updrafts were primarily in the DSL quadrant

References

Aberson, S. D., M. T. Montgomery, M. Bell, and M. Black, 2006: Hurricane Isabel (2003): New insights into the physics of intense storms. Part II. *Bull. Amer. Meteor. Soc.*, **87**, 1349–1354, doi:10.1175/BAMS-87-10-1349.

Berg, R., 2016a: Hurricane Joaquin. *NHC Trop. Cycl. Rep. AL112015*, 36 pp., URL http://www.nhc.noaa.gov/data/tcr/AL112015_Joaquin.pdf.

Berg, R., 2016b: Hurricane Marty. *NHC Trop. Cycl. Rep. EP172015*, 17 pp., URL http://www.nhc.noaa.gov/data/tcr/EP172015_Marty.pdf.

Black, M. L., R. W. Burpee, and F. D. M. Jr., 1996: Vertical motion characteristics of tropical cyclones determined with airborne Doppler radial velocities. *J. Atmos. Sci.*, **53**, 1887–1909.

Black, M. L., J. F. Gamache, F. D. M. Jr., C. E. Samsury, and H. E. Willoughby, 2002: Eastern Pacific Hurricanes Jimena of 1991 and Olivia of 1994: The effect of vertical shear on structure and intensity. *Mon. Wea. Rev.*, **130**, 2291–2312.

Black, P., L. Harrison, M. Beaubien, R. Bluth, R. Woods, A. Penny, R. Smith, and J. Doyle, 2016: High Definition Sounding System (HDSS) for atmospheric profiling. *J. Atmos. Oceanic Technol.*, **in press**, doi:10.1175/JTECH-D-14-00210.1.

Black, R. A., H. B. Bluestein, and M. L. Black, 1994: Unusually strong vertical motions in a Caribbean hurricane. *Mon. Wea. Rev.*, **122**, 2722–2739.

Braun, S. A., M. T. Montgomery, and Z. A. Pu, 2006: High-resolution simulation of hurricane Bonnie (1998). Part I: The organization of eyewall vertical motion. *J. Atmos. Sci.*, **63**, 19–42.

Corbosiero, K. L., and J. Molinari, 2002: The effects of vertical wind shear on the distribution of convection in tropical cyclones. *Mon. Wea. Rev.*, **130**, 2110–2123.

Corbosiero, K. L., and J. Molinari, 2003: The relationship between storm motion, vertical wind shear, and convective asymmetries in tropical cyclones. *J. Atmos. Sci.*, **60**, 366–376.

Corbosiero, K. L., J. Molinari, A. R. Aiyyer, and M. L. Black, 2006: The structure and evolution of Hurricane Elena (1985). Part II: Convective asymmetries and evidence for vortex Rossby waves. *Mon. Wea. Rev.*, **134**, 3073–3091, doi:10.1175/MWR3250.1.

Creasey, R. L., and R. L. Elsberry, 2016: Tropical cyclone center positions from sequences of HDSS sondes deployed along high-altitude overpasses. *Submitted to Wea. Forecasting*, 1–25.

DeHart, J. C., R. A. H. Jr., and R. F. Rogers, 2014: Quadrant distribution of tropical cyclone inner-core kinematics in relation to environmental shear. *J. Atmos. Sci.*, **71**, 2713–2732, doi:10.1175/JAS-D-13-0298.1.

DeMaria, M., R. T. DeMaria, J. A. Knaff, and D. Molenar, 2012: Tropical cyclone lightning and rapid intensity change. *Mon. Wea. Rev.*, **140**, 1828–1842.

DeMaria, M., and J. Kaplan, 1994: A statistical hurricane intensity prediction scheme (SHIPS) for the Atlantic basin. *Wea. Forecasting*, **9**, 209–220.

Ditchek, S. D., and J. Molinari, 2016: The composited tropical cyclone outflow layer and the balanced vortex response. *32nd Conference on Hurricanes and Tropical Meteorology*, URL https://ams.confex.com/ams/32Hurr/webprogram/Manuscript/Paper292790/HTM32_Ditchek_ExtendedAbstract.pdf.

Franklin, J. L., S. J. Ford, S. E. Feuer, and F. D. M. Jr., 1993: The kinematic structure of Hurricane Gloria (1985) determined from nested analyses of dropwindsonde and Doppler radar data. *Mon. Wea. Rev.*, **121**, 2433–2451.

Guimond, S. R., G. M. Heymsfield, and F. J. Turk, 2010: Multiscale observations of Hurricane Dennis (2005): The effects of hot towers on rapid intensification. *J. Atmos. Sci.*, **67**, 633–654, doi:10.1175/2009JAS3119.1.

Heymsfield, G. M., L. Tian, A. J. Heymsfield, L. Li, and S. Guimond, 2010: Characteristics of deep tropical and subtropical convection from nadir-viewing high-altitude airborne Doppler radar. *J. Atmos. Sci.*, **67**, 285–308, doi:10.1175/2009JAS3132.1.

Hock, T. F., and J. L. Franklin, 1999: The NCAR GPS dropwindsonde. *Bull. Amer. Meteor. Soc.*, **80**, 407–420.

Jorgensen, D. P., E. J. Zipser, and M. A. LeMone, 1985: Vertical motions in intense hurricanes. *J. Atmos. Sci.*, **42**, 839–856.

Kaplan, J., and M. DeMaria, 2003: Large-scale characteristics of rapidly intensifying tropical cyclones in the North Atlantic basin. *Wea. Forecasting*, **18**, 1093–1108.

Kimberlain, T. B., E. S. Blake, and J. P. Cangialosi, 2016: Hurricane Patricia. *NHC Trop. Cycl. Rep. EP202015*, 32 pp., URL http://www.nhc.noaa.gov/data/tcr/EP202015_Patricia.pdf.

Marks, F. D., P. G. Black, M. T. Montgomery, and R. W. Burpee, 2008: Structure of the eye and eyewall of Hurricane Hugo (1989). *Mon. Weather Rev.*, **136**, 1237–1259.

Moon, Y., and D. S. Nolan, 2015: Spiral rainbands in a numerical simulation of Hurricane Bill (2009). Part II: Propagation of inner rainbands. *J. Atmos. Sci.*, **72**, 191–215, doi:10.1175/JAS-D-14-0056.1.

Pasch, R. J., 2011: Hurricane intensity forecast improvement: is it possible. *National Hurricane Conference*, URL http://www.nhc.noaa.gov/outreach/presentations/2011_IntensityForecastingImprovement_Pasch.pdf.

Persing, J., and M. T. Montgomery, 2003: Hurricane superintensity. *J. Atmos. Sci.*, **60**, 2349–2371.

Reasor, P. D., R. Rogers, and S. Lorsolo, 2013: Environmental flow impacts on tropical cyclone structure diagnosed from airborne Doppler radar composites. *Mon. Wea. Rev.*, **141**, 2949–2969, doi:10.1175/MWR-D-12-00334.1.

Rogers, R., S. Lorsolo, P. Reasor, J. Gamache, and F. Marks, 2012: Multiscale analysis of tropical cyclone kinematic structure from airborne Doppler radar composites. *Mon. Wea. Rev.*, **140**, 77–99, doi:10.1175/MWR-D-10-05075.1.

Shapiro, L. J., and H. E. Willoughby, 1982: The response of balanced hurricanes to local sources of heat and momentum. *J. Atmos. Sci.*, **39**, 378–394.

Stern, D. P., and S. D. Aberson, 2006: Extreme vertical winds measured by dropwindsondes in hurricanes. *27th Conf. on Hurricanes and Tropical Meteorology*.

Stern, D. P., G. H. Bryan, and S. D. Aberson, 2016: Extreme low-level updrafts and wind speeds measured by dropsondes in tropical cyclones. *Mon. Wea. Rev.*, **144**, 2177–2204, doi:10.1175/MWR-D-15-0313.1.

Stern, D. P., J. L. Vigh, and D. S. Nolan, 2015: Revisiting the relationship between eyewall contraction and intensification. *J. Atmos. Sci.*, **72**, 1283–1306, doi:10.1175/JAS-D-14-0261.1.

Vaisala, 2010: Vaisala dropsonde RD94. *Vaisala Rep., 2 pp.*, URL http://www.vaisala.com/Vaisala%20Documents/Brochures%20and%20Datasheets/RD94-Dropsonde-Datasheet-B210936EN-A-LoRes.pdf.

Wang, J., J. Bian, W. O. Brown, H. Cole, V. Grubii, and K. Young, 2009: Vertical air motion from T-REX radiosonde and dropsonde data. *J. Atmos. Oceanic Technol.*, **26**, 928–942, doi:10.1175/2008JTECHA1240.1.

Wang, J., and Coauthors, 2015: A long-term, high-quality, high-vertical-resolution GPS dropsonde dataset for hurricane and other studies. *Bull. Amer. Meteor. Soc.*, **96**, 961–973, doi:10.1175/BAMS-D-13-00203.1.

Willoughby, H. E., and M. B. Chemlow, 1982: Objective determination of hurricane tracks from aircraft observations. *Mon. Wea. Rev.*, **110**, 1298–1305.

Bonus Slides

Discussion

- Distinguishing the altitudinal, azimuthal, and radial tendencies for moderate, strong, and extreme UDs plays a crucial role in:
  - Understanding how shear interacts with TCs
  - TC intensity changes
- Conducted using XDD Dropsondes in Marty, Joaquin, and Patricia (2015)
- Extension of Stern et al. (2016) and Stern and Aberson (2006), which only had data in lowest 2 – 3 km
  - Most comparable studies to this current work

Discussion

- Distinguishing the altitudinal, azimuthal, and radial tendencies for moderate, strong, and extreme UDs plays a crucial role in:
  - Understanding how shear interacts with TCs
  - TC intensity changes
- Conducted using XDD Dropsondes in Marty, Joaquin, and Patricia (2015)
- Extension of Stern et al. (2016) and Stern and Aberson (2006), which only had data in lowest 2 – 3 km
  - Most comparable studies to this current work

Discussion

- Distinguishing the altitudinal, azimuthal, and radial tendencies for moderate, strong, and extreme UDs plays a crucial role in:
  - Understanding how shear interacts with TCs
  - TC intensity changes
- Conducted using XDD Dropsondes in Marty, Joaquin, and Patricia (2015)
- Extension of Stern et al. (2016) and Stern and Aberson (2006), which only had data in lowest 2 – 3 km
  - Most comparable studies to this current work

TC Intensity

- Moderate, strong and extreme UDs occurred in weak and strong TCs and in different shear environments
  - Some correlation between convection (via gamma parameter) and intensity
    - Positive gamma peaks before intensification
  - Percent of updrafts and moderate downdrafts inside the RMW increased before intensification

TC Intensity

- Moderate, strong and extreme UDs occurred in weak and strong TCs and in different shear environments
  - Some correlation between convection (via gamma parameter) and intensity
    - Positive gamma peaks before intensification
  - Percent of updrafts and moderate downdrafts inside the RMW increased before intensification

TC Intensity

- Moderate, strong and extreme UDs occurred in weak and strong TCs and in different shear environments
  - Some correlation between convection (via gamma parameter) and intensity
    - Positive gamma peaks before intensification
  - Percent of updrafts and moderate downdrafts inside the RMW increased before intensification

Convection Locations

- Occurred both inside and outside the RMW, but decreased in strength outside of “inner core”
  - Collectively, majority of moderate, strong, and extreme convection was outside of RMW
- Outside of inner core, periodic pattern of convection
- Vertical velocities maximized in strength:
  - Aloft near 12 km (Jorgensen et al. 1985; Marks et al. 2008; Rogers et al. 2012)
  - Just above the surface (Stern et al. 2016)

Convection Locations

- Occurred both inside and outside the RMW, but decreased in strength outside of “inner core”
  - Collectively, majority of moderate, strong, and extreme convection was outside of RMW
- Outside of inner core, periodic pattern of convection
- Vertical velocities maximized in strength:
  - Aloft near 12 km (Jorgensen et al. 1985; Marks et al. 2008; Rogers et al. 2012)
  - Just above the surface (Stern et al. 2016)

Convection Locations

- Occurred both inside and outside the RMW, but decreased in strength outside of “inner core”
  - Collectively, majority of moderate, strong, and extreme convection was outside of RMW
- Outside of inner core, periodic pattern of convection
- Vertical velocities maximized in strength:
  - Aloft near 12 km (Jorgensen et al. 1985; Marks et al. 2008; Rogers et al. 2012)
  - Just above the surface (Stern et al. 2016)

Convection Locations

- Updrafts tended to maximize in strength:
  - DSL quadrant inside 1.75R* (Black et al. 2002; Corbosiero and Molinari 2002, 2003; Stern and Aberson 2006; Guimond et al. 2010; Reasor et al. 2013)
  - DSR and USL quadrants between 1.75R* and 3R*
  - USL and (small spot in the USR) quadrant at outer radii (Corbosiero and Molinari 2002, 2003; DeHart et al. 2014)
- Suppressed updrafts through most of the USR quadrant
- Downdrafts tended to maximize in strength:
  - DSR quadrant inside 1.75R*
  - USR and USL quadrants between 1.75R* and 3R*
  - DSL quadrant at outer radii

Convection Locations

- Updrafts tended to maximize in strength:
  - DSL quadrant inside 1.75R* (Black et al. 2002; Corbosiero and Molinari 2002, 2003; Stern and Aberson 2006; Guimond et al. 2010; Reasor et al. 2013)
  - DSR and USL quadrants between 1.75R* and 3R*
  - USL and (small spot in the USR) quadrant at outer radii (Corbosiero and Molinari 2002, 2003; DeHart et al. 2014)
- Suppressed updrafts through most of the USR quadrant
- Downdrafts tended to maximize in strength:
  - DSR quadrant inside 1.75R*
  - USR and USL quadrants between 1.75R* and 3R*
  - DSL quadrant at outer radii

Convection Locations

- Updrafts tended to maximize in strength:
  - DSL quadrant inside 1.75R* (Black et al. 2002; Corbosiero and Molinari 2002, 2003; Stern and Aberson 2006; Guimond et al. 2010; Reasor et al. 2013)
  - DSR and USL quadrants between 1.75R* and 3R*
  - USL and (small spot in the USR) quadrant at outer radii (Corbosiero and Molinari 2002, 2003; DeHart et al. 2014)
- Suppressed updrafts through most of the USR quadrant
- Downdrafts tended to maximize in strength:
  - DSR quadrant inside 1.75R*
  - USR and USL quadrants between 1.75R* and 3R*
  - DSL quadrant at outer radii

Future Work

- Examine the sources of these moderate, strong and extreme UDs
  - 37 GHz polarization correction temperature microwave data and satellite data (Naval Research Laboratory)
  - Moisture and buoyancy
  - Bulk Richardson number
  - CAPE
  - Sea surface temperature
  - Potentially, modeling initialized on soundings
- Differentiating between inner core convection and inner rainband convection
- Evaluate the strength of the updraft cores in relation to the secondary circulation

Future Work

- Examine the sources of these moderate, strong and extreme UDs
  - 37 GHz polarization correction temperature microwave data and satellite data (Naval Research Laboratory)
  - Moisture and buoyancy
  - Bulk Richardson number
  - CAPE
  - Sea surface temperature
  - Potentially, modeling initialized on soundings
- Differentiating between inner core convection and inner rainband convection
- Evaluate the strength of the updraft cores in relation to the secondary circulation

Future Work

- Examine the sources of these moderate, strong and extreme UDs
  - 37 GHz polarization correction temperature microwave data and satellite data (Naval Research Laboratory)
  - Moisture and buoyancy
  - Bulk Richardson number
  - CAPE
  - Sea surface temperature
  - Potentially, modeling initialized on soundings
- Differentiating between inner core convection and inner rainband convection
- Evaluate the strength of the updraft cores in relation to the secondary circulation

Date	Storm	I [m s^{-1}]	N_t	|S| [m s^{-1}]	S_D [deg]
27 Sept	Marty	25.72	50	11.21	98
28 Sept	Marty	36.01	62	11.00	89
2 Oct	Joaquin	56.59	75	4.90	151
3 Oct	Joaquin	66.88	65	13.20	127
4 Oct	Joaquin	43.73	66	4.90	66
5 Oct	Joaquin	38.58	76	3.90	39
20 Oct	Patricia	15.43	12	5.25	42
21 Oct	Patricia	25.72	51	2.93	195
22 Oct	Patricia	59.16	63	0.62	146
23 Oct	Patricia	92.60	7	4.58	21
TOTAL	----------	**46.04 (avg)**	**5 0**	**6.25 (avg)**	----------

- 590 Sondes Total
- Previous studies of sonde calculated vertical velocities achieve this in 30+ Storms (e.g., Stern et al. 2016)
- With ~700 data points per sonde, that's approximately 413,000 data points

Date	Storm	I [m s^{-1}]	N_t	|S| [m s^{-1}]	S_D [deg]
27 Sept	Marty	25.72	50	11.21	98

- Strongly sheared
- Maximum observed strength = Cat. 1
- Westerly shear
- 112 Sondes Total

23 Oct	Patricia	92.60	70	4.58	21
TOTAL	**----------**	**46.04 (avg)**	**590**	**6.25 (avg)**	**----------**

Date	Storm	I [m s^{-1}]	N_t	|S| [m s^{-1}]	S_D
28 Sept	Marty	36.01	62	11.00	89
2 Oct	Joaquin	56.59	75	4.90	151
3 Oct	Joaquin	66.88	65	13.20	127

- Moderately sheared
- Maximum observed strength = Cat. 4
- Northwesterly to Southwesterly shear
- 282 Sondes Total

TOTAL	**----------**	**46.04 (avg)**	**590**	**6.25 (avg)**	**----------**

Date	Storm	I [m s^{-1}]	N_t	|S| [m s^{-1}]	S_D [ ]

- Weakly sheared
- Maximum observed strength = Cat. 5
- Southwesterly to Northwesterly shear**
- 196 Sondes Total

4 Oct	Joaquin	43.73	66	4.90	66
5 Oct	Joaquin	38.58	76	3.90	39
20 Oct	Patricia	15.43	12	5.25	42
21 Oct	Patricia	25.72	51	2.93	195
TOTAL	**----------**	**46.04 (avg)**	**590**	**6.25 (avg)**	**----------**

Percent of Total Sondes above Threshold

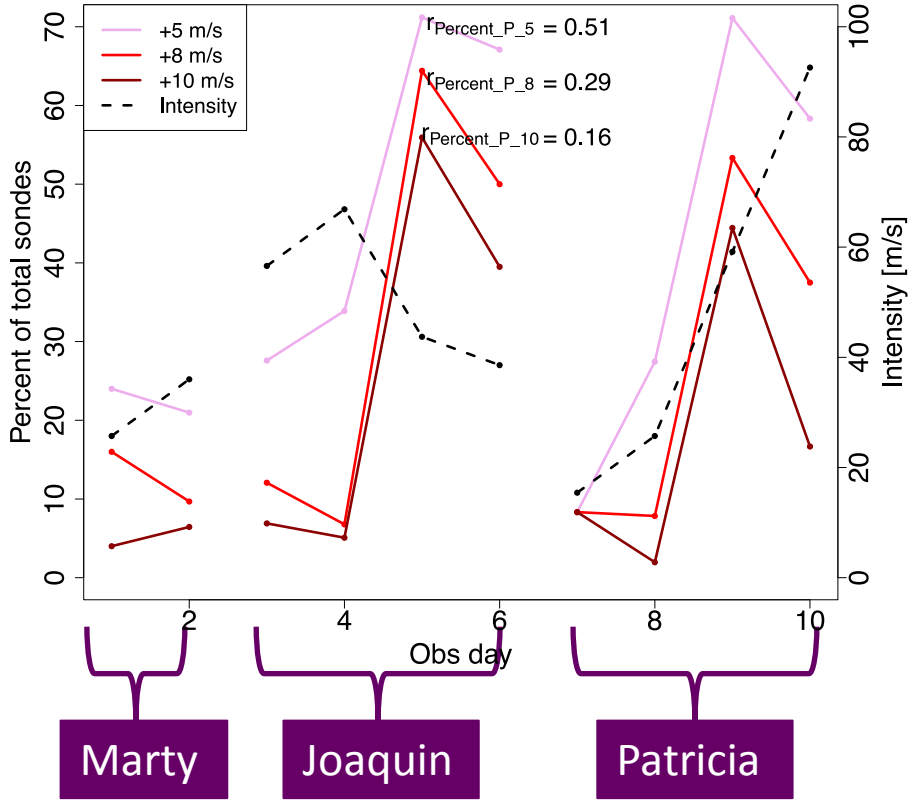

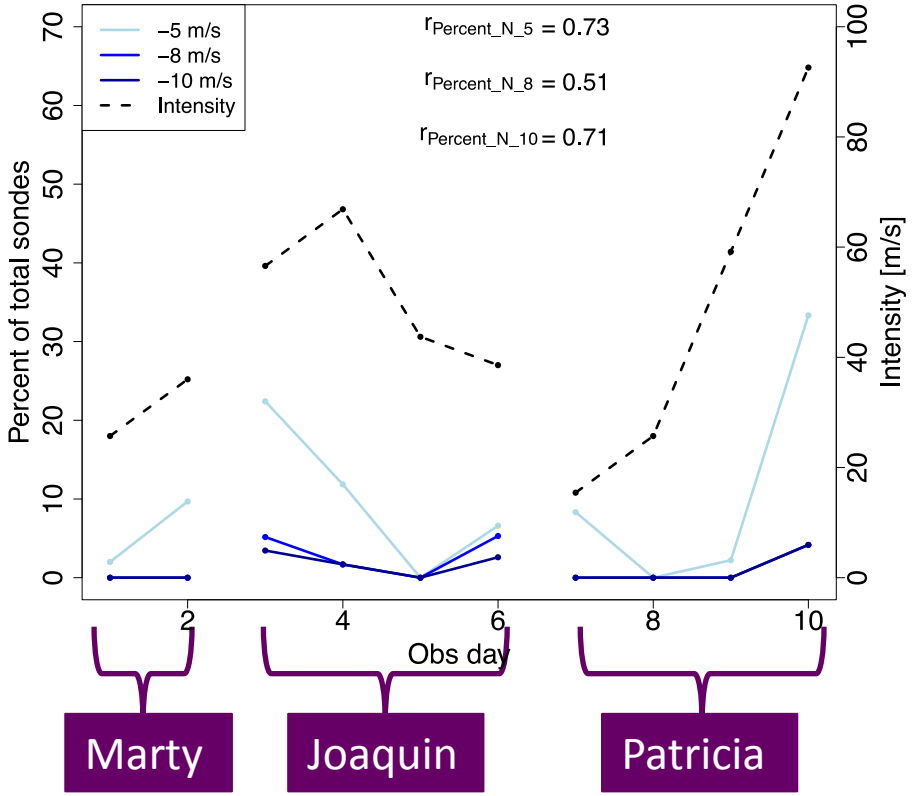

Percent of Total Sondes above Threshold

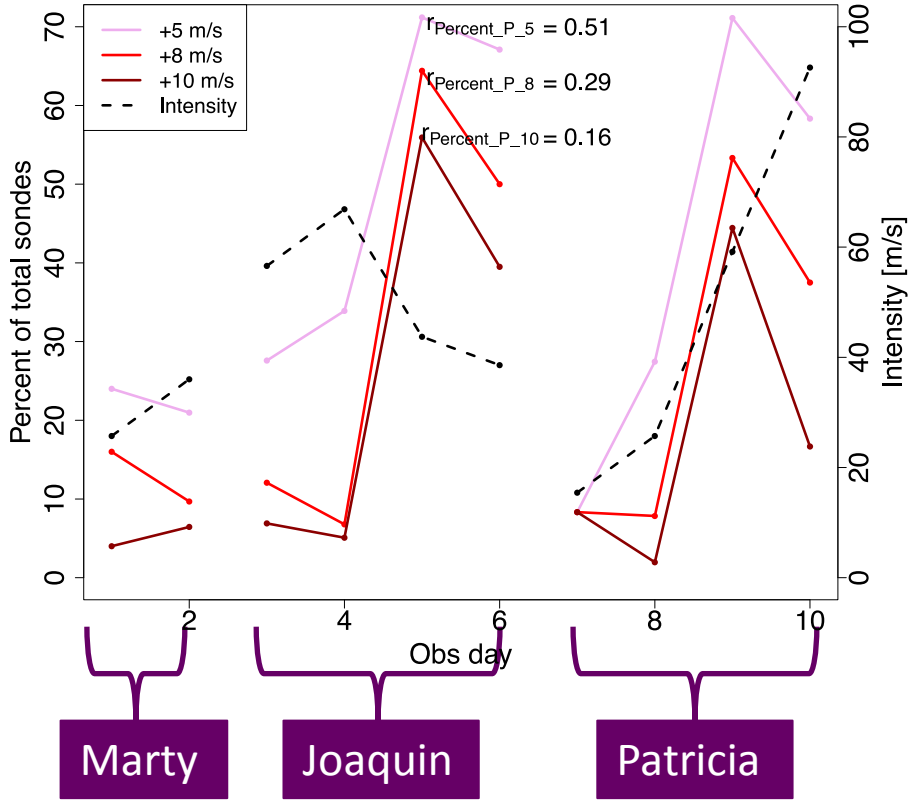

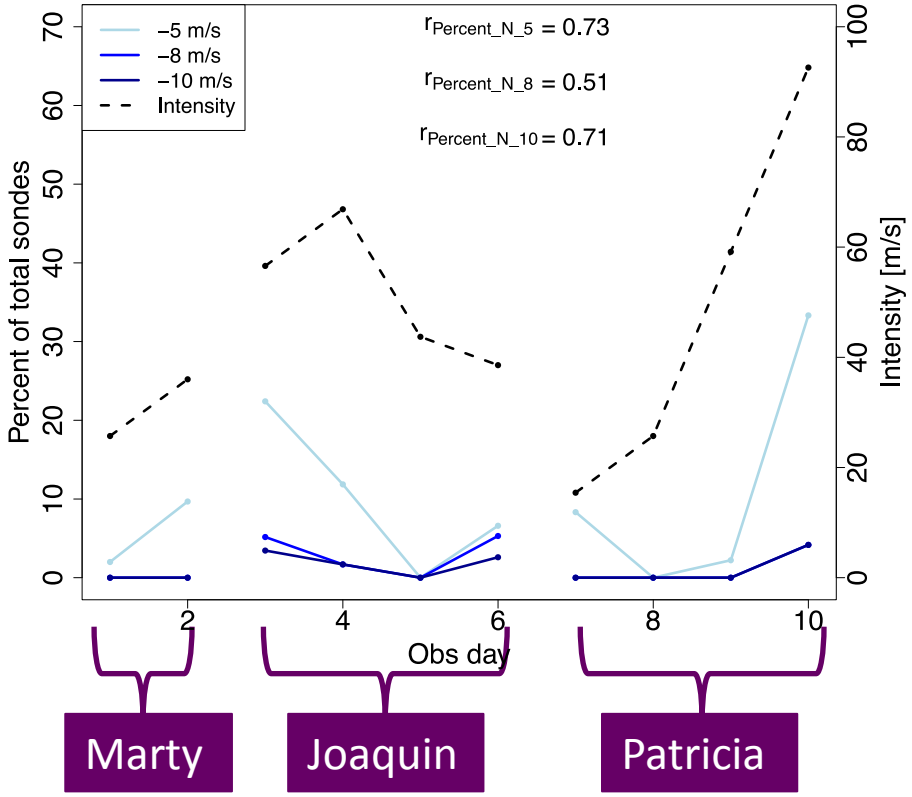

- Not a clear relationship between intensity and percent of total sondes
- Maximum Correlations: Positive: +5 m s^{-1} at 0.51
  Negative: - 5 m s^{-1} at 0.73

Filtered Data Example

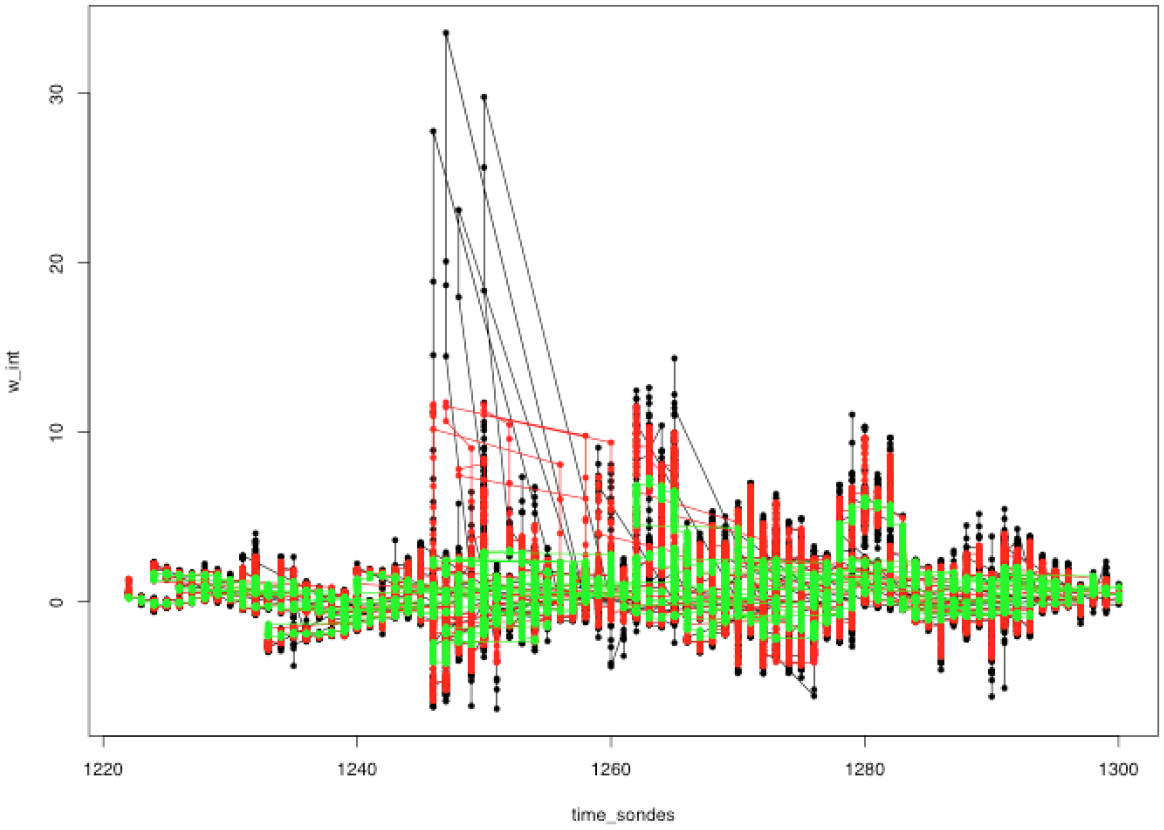

- Example of filtering of data: Marty on 27 Sept. 2015
- Black is raw data
- Red is nine-point binomial filter
- Green is 100 Hz Butter filter that has been corrected for phase shift

Calculating the TC Center

- Take the NHC Best-Track TC center as initial ‘guess’
  - Linearly interpolated to the minute
- Compute orthogonal lines from pairs of wind observations following Creasey and Elsberry (2016) and Willoughby and Chelmow (1982)
  - Wind speeds are motion corrected by subtracting the NHC Best-Track motion
- Take the weighted mean of the intersections of all pairs of the orthogonal lines
- Weighting function follows a power law

$$W = V_t/d^2$$

- Where V_t is the tangential wind speed and d is the mean distance of the pairs to the initial guess
- Produces a ‘wind field corrected’ mean Best-Track center for the duration of the flight into a TC

Example

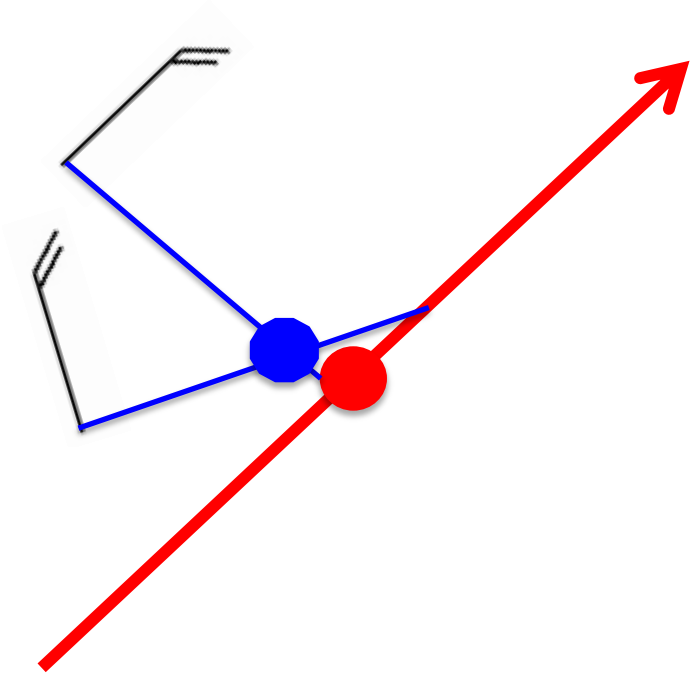

- Red line is the NHC Best-Track center linearly interpolated to the minute
- Red dot is the average NHC Best-Track center between Obs 1 and Obs 2 (wind barbs)
- Blue lines are orthogonal to wind barbs
- Blue dot is intersection

Example

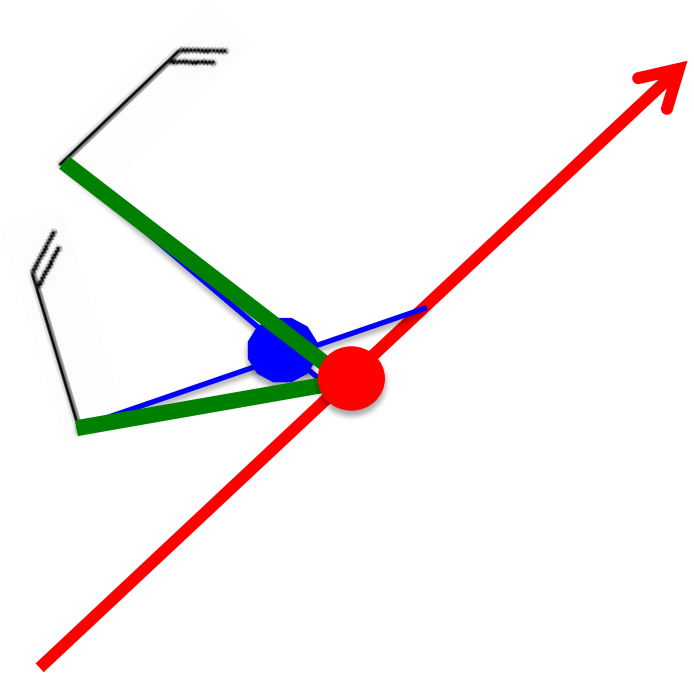

- The weighting function is the mean tangential wind speed of the two points divided by the mean distance of the two observations from the NHC Best Track center (green) at that time, squared

Example

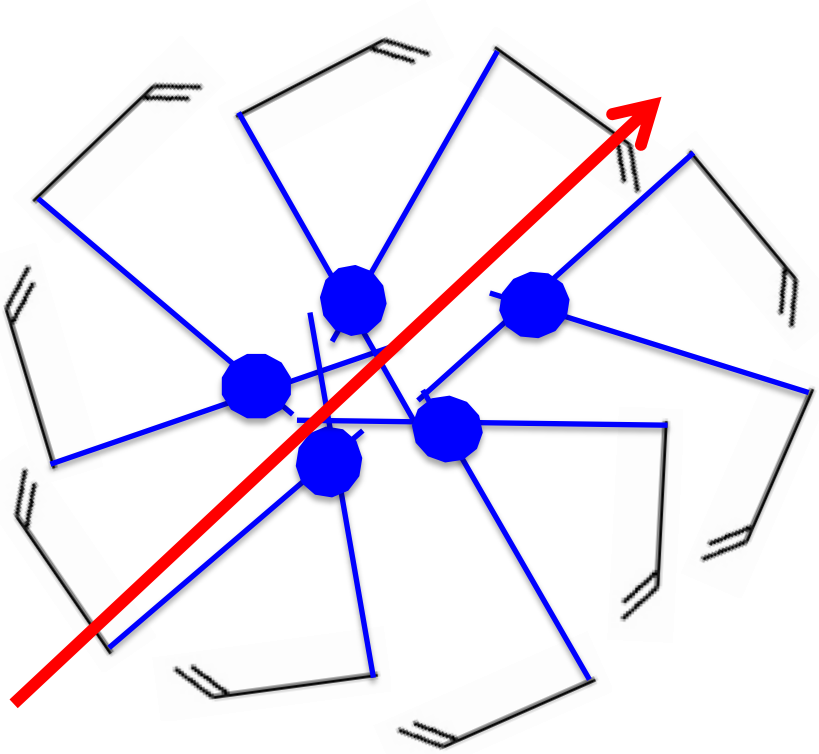

- Given many pairs over the entire observation period of a TC, not just a transect, which may or may not go over the center, a MEAN wind corrected TC center can be obtained

Real World Example

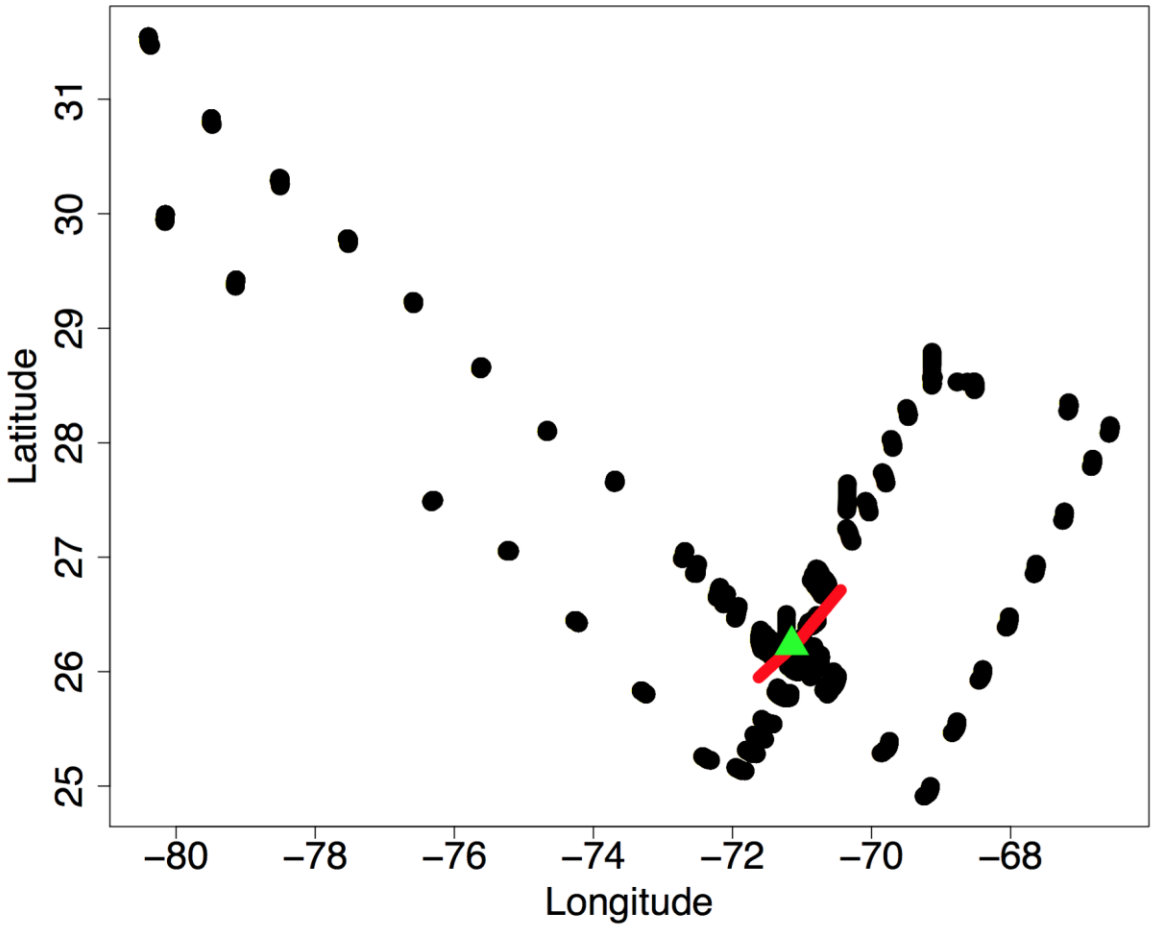

Surface Fall Speed Factor

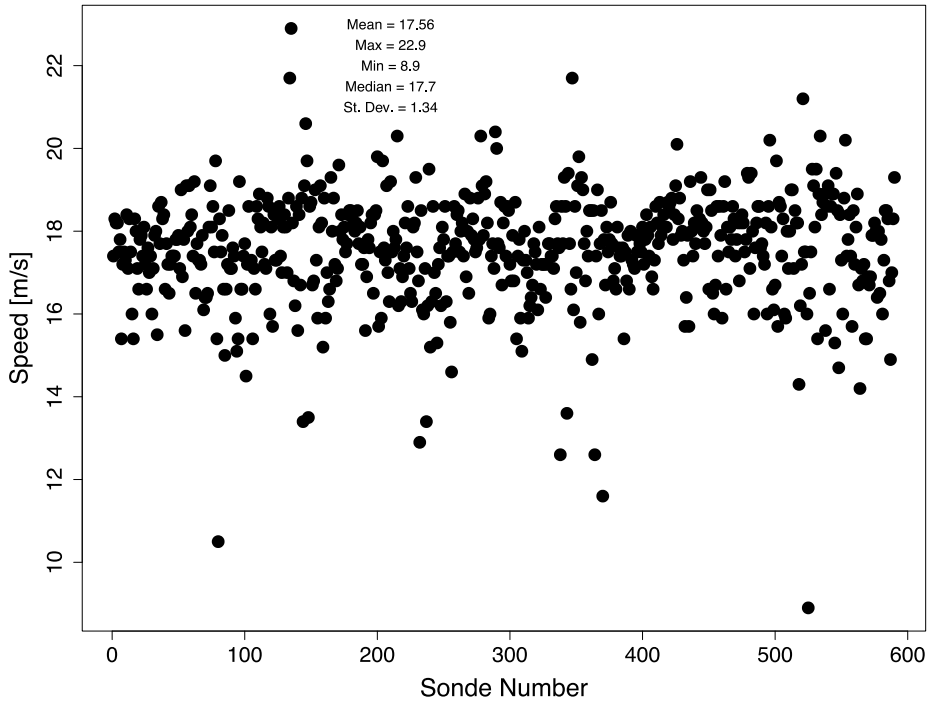

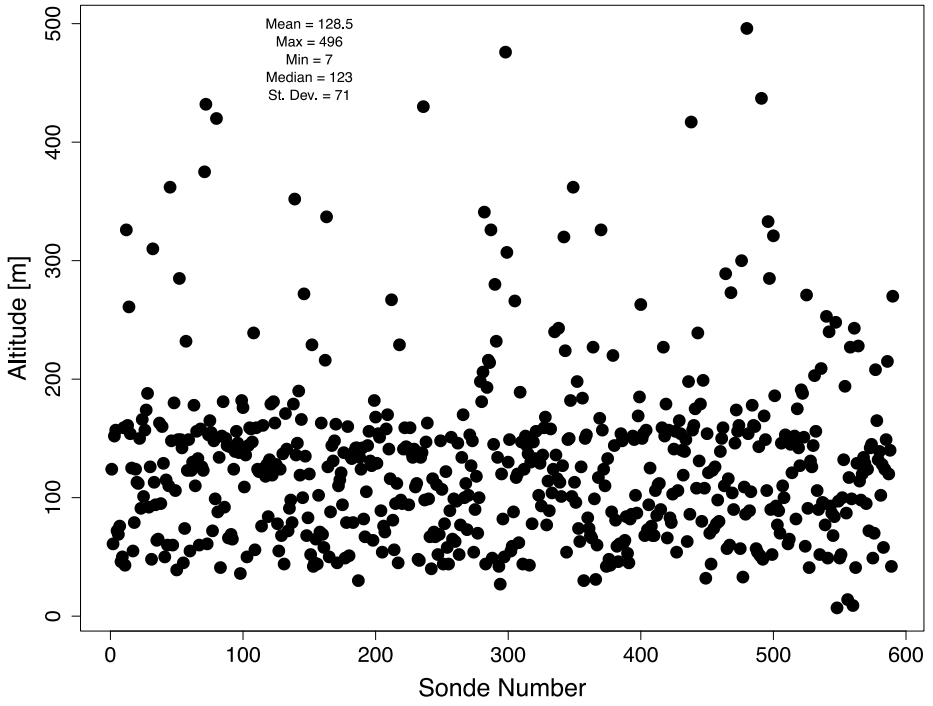

Surface Fall Speed Factor

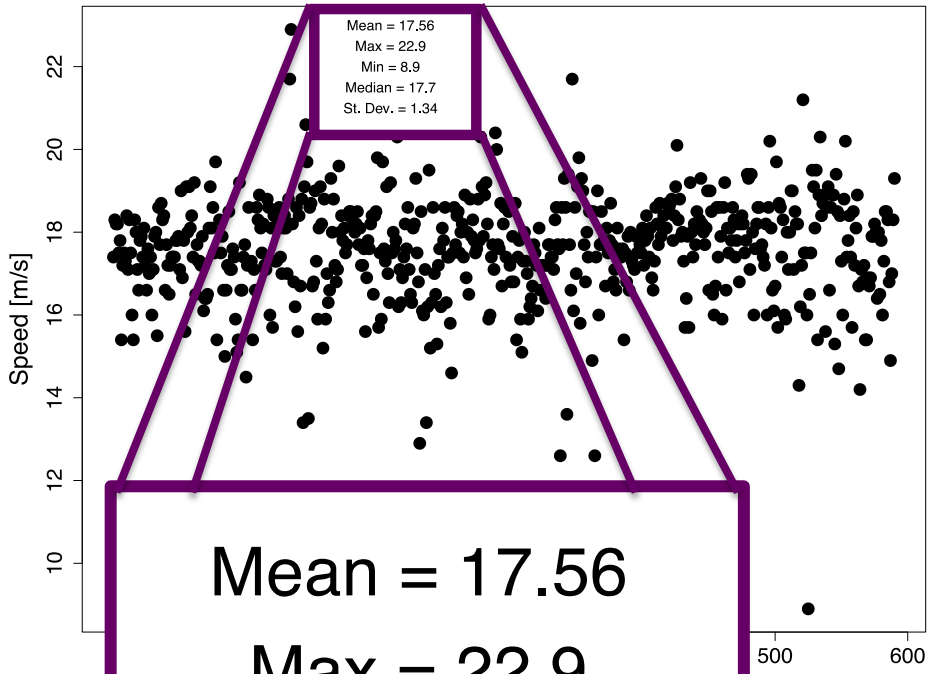

Mean = 17.56

Max = 22.9

Min = 8.9

Median = 17.7

St. Dev. = 1.34

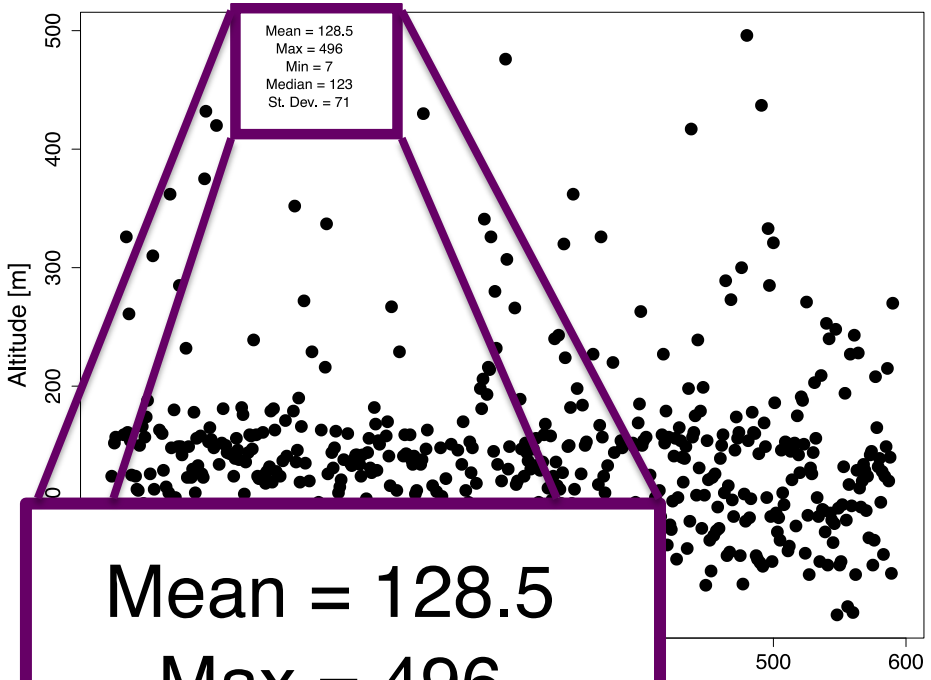

Mean = 128.5

Max = 496

Min = 7

Median = 123

St. Dev. = 71

Surface Fall Speed Factor

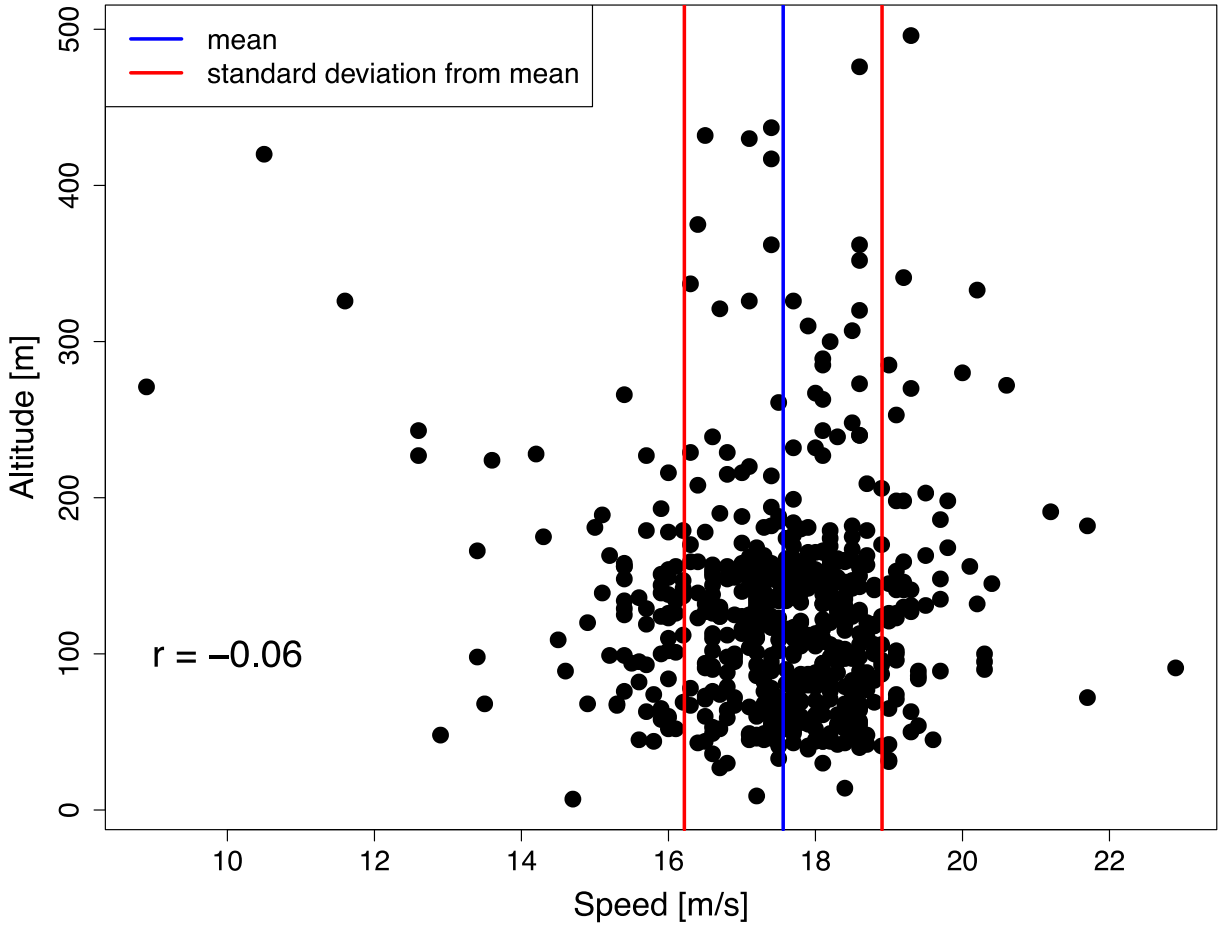

- Very weak (and negative) correlation between height of “surface” and the fall speed
- Most data within 1 standard deviation of mean fall speed
- Outside of 1 standard deviation not affected by altitude
- Close to the 18 m s^{-1} surface fall speed reported by Black et al. (2016)

Quadrant Analysis

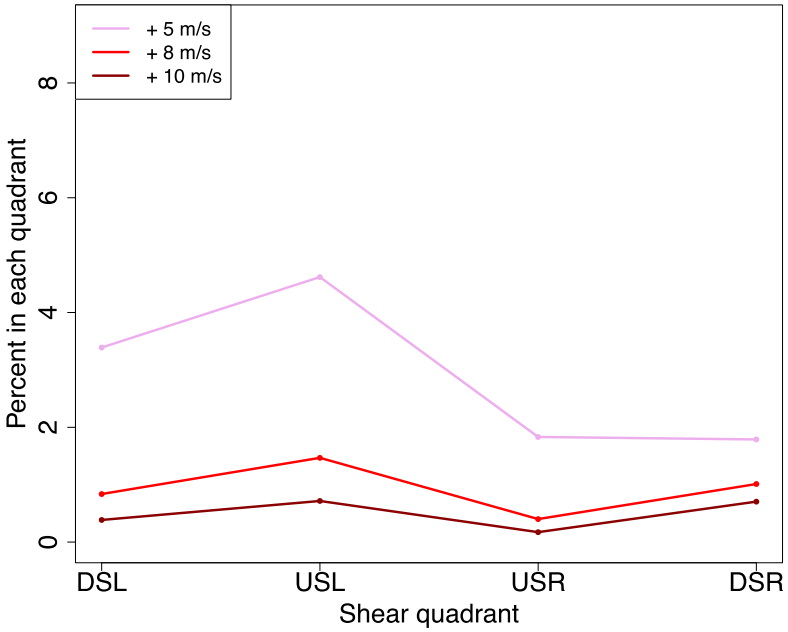

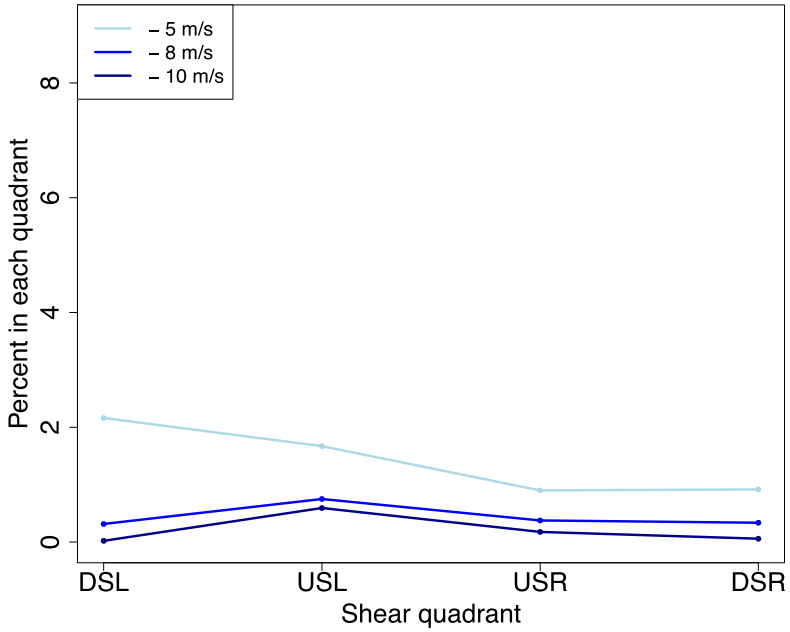

- Summing over each quadrant and all radii up to R* = 10…
  - Updrafts maximized in occurrence in the USL quadrant with a secondary maxima in the DSR quadrant
  - Downdrafts occurred less frequently, but there were peaks in the DSL (moderate), USL (strong and extreme)

Quadrant Analysis

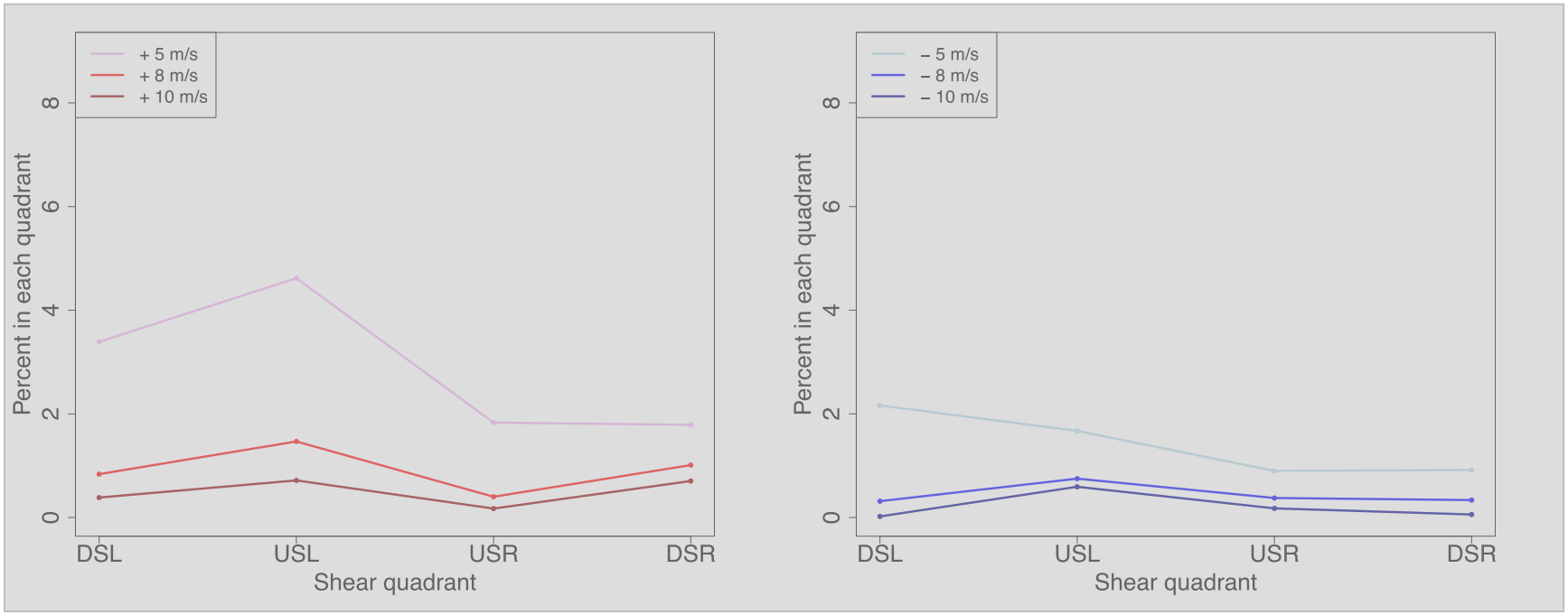

Quadrant Analysis

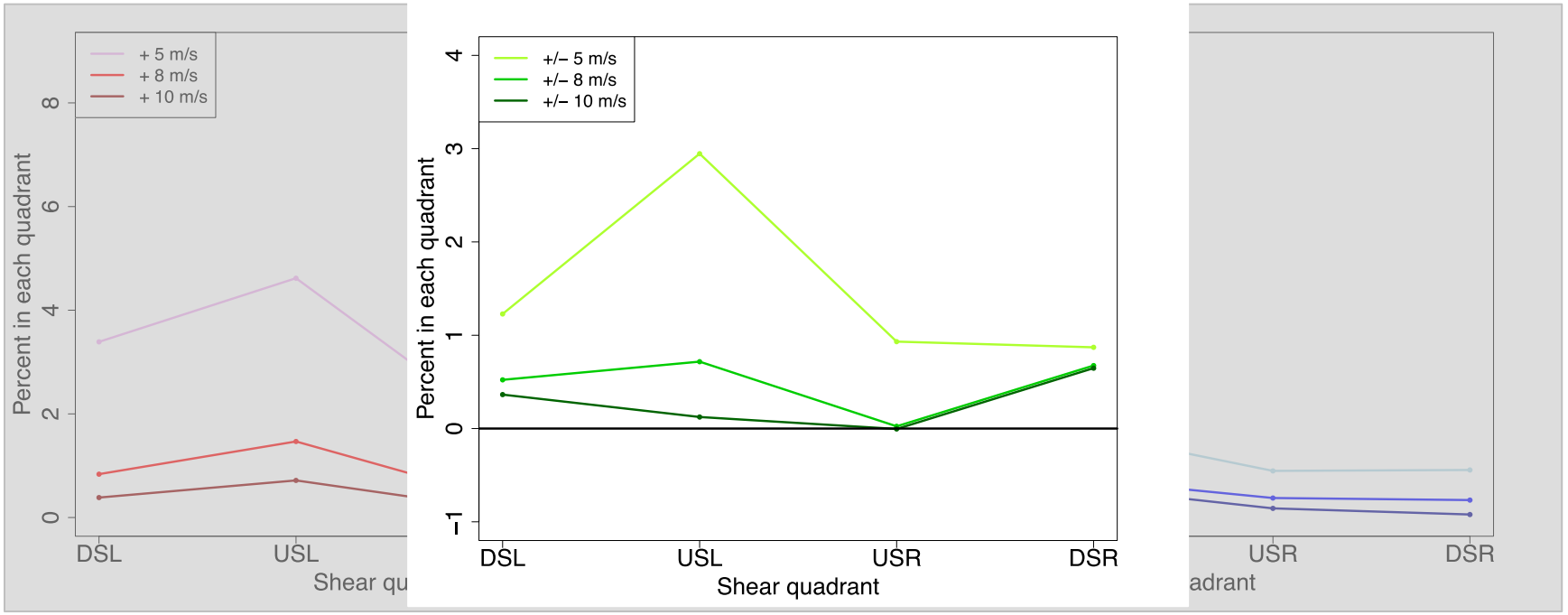

- Subtracting updrafts and downdrafts…
  - Moderate updrafts dominated the USL quadrant, strong and extreme updrafts dominated the DSR
  - Downdrafts dominated the USR quadrant

Quadrant Analysis: Inner Core

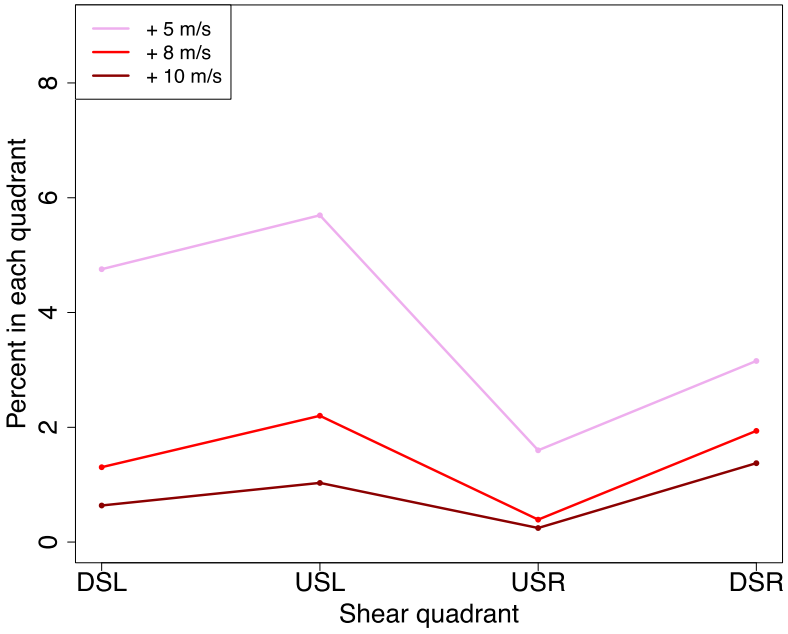

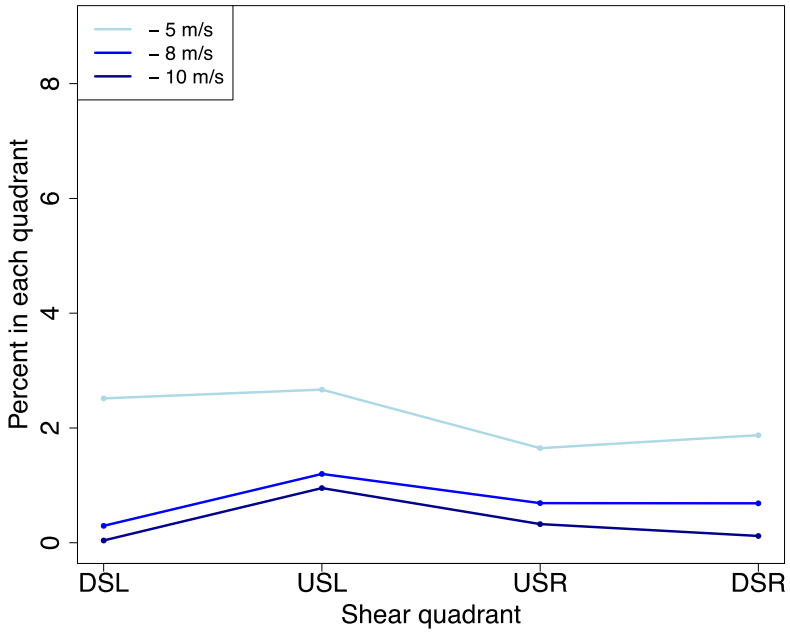

- Restricting to the inner core (3R*)…
  - Updrafts still maximized in occurrence in the USL and DSR quadrants
  - Downdrafts maximized in occurrence in the USL
    - Fits previous ‘helical rise’ theory

Quadrant Analysis: Inner Core

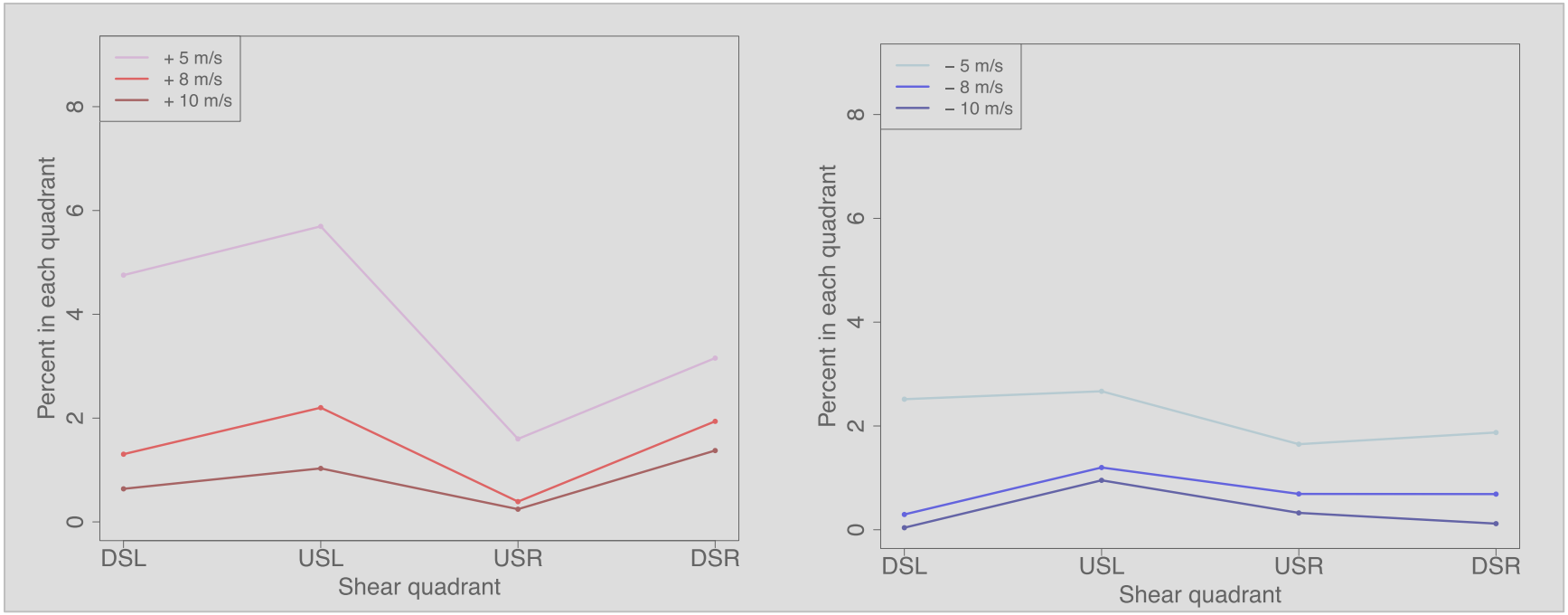

Quadrant Analysis: Inner Core

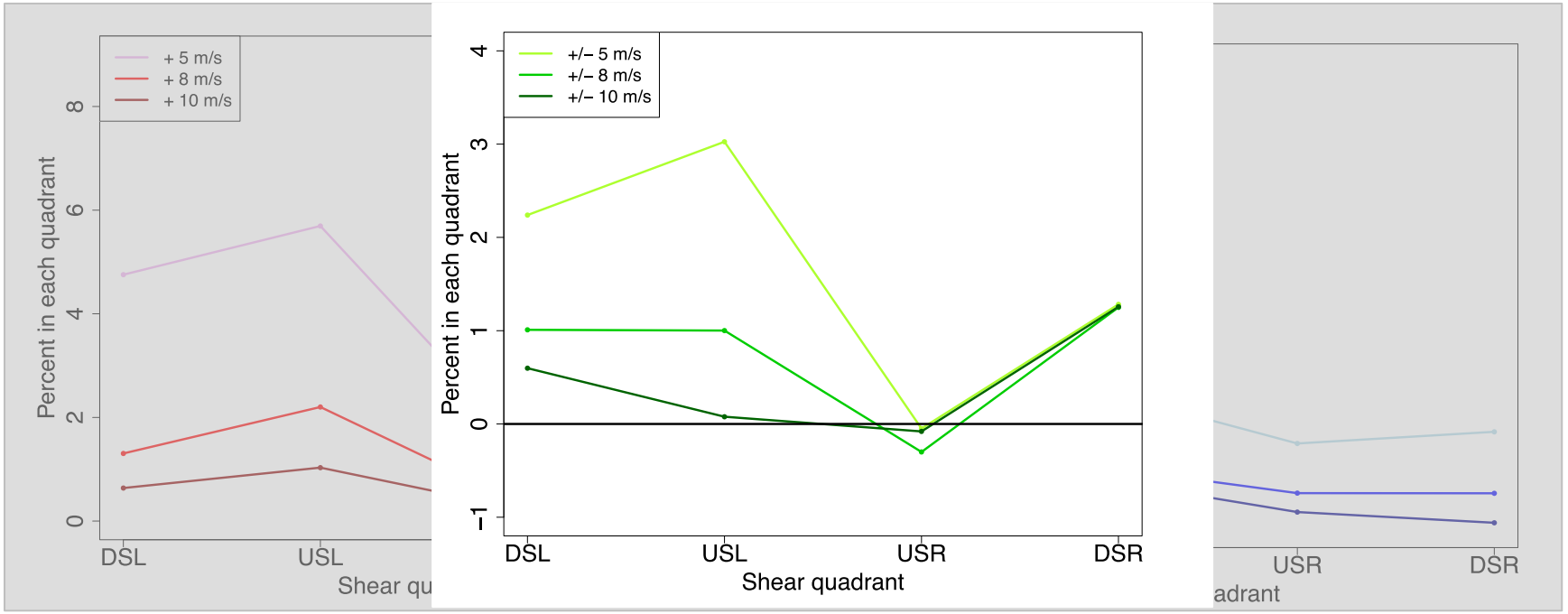

- Subtracting updrafts and downdrafts…
  - Moderate updrafts dominated the USL quadrant, strong and extreme dominated the DSR quadrant
  - Downdrafts dominated the USR quadrant
- SAME QUALITATIVE RESULTS AS THE FULL DATASET!!!!

Are the near-surface updrafts error?

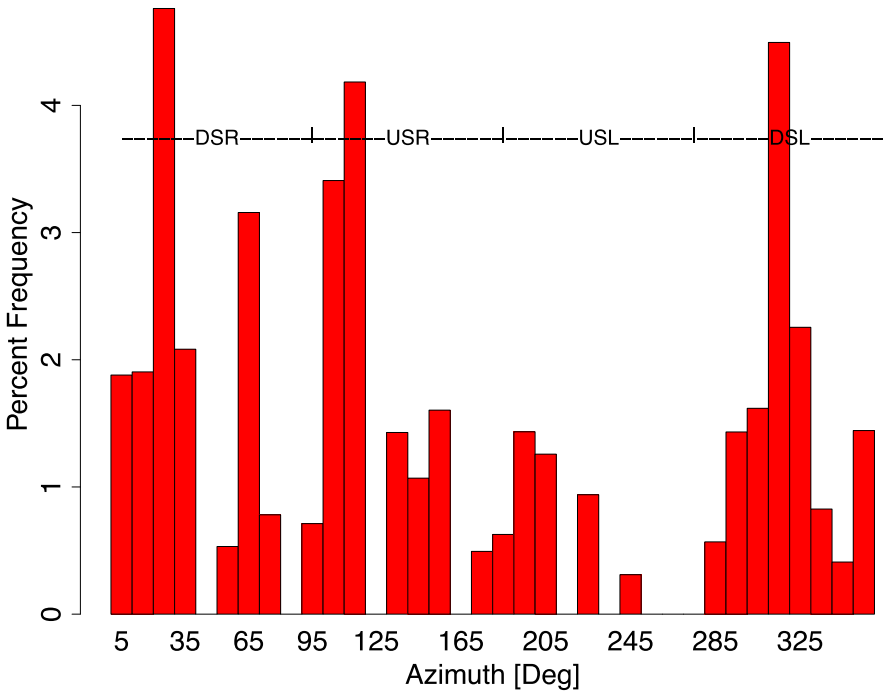

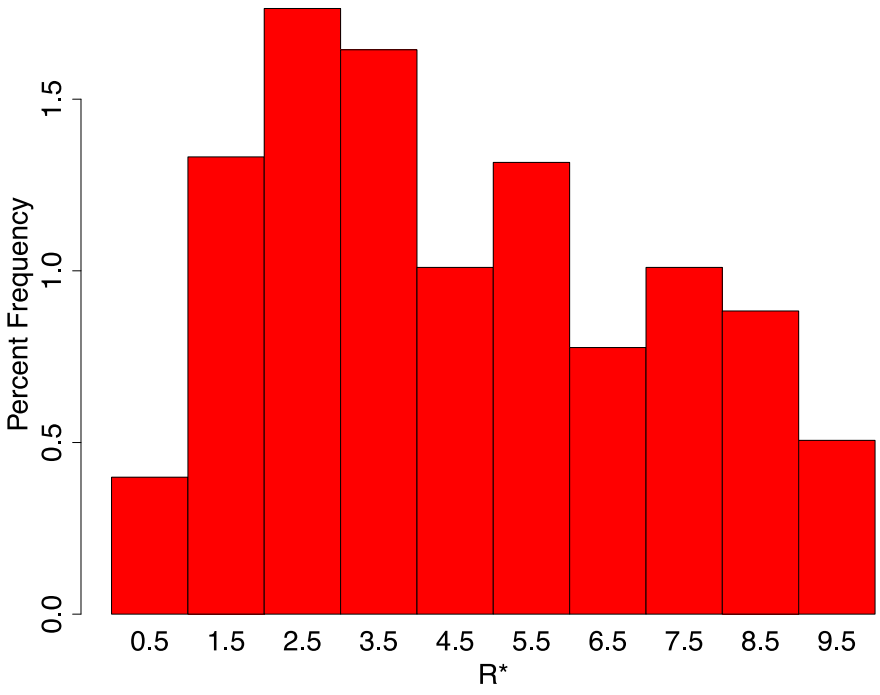

- If near-surface updrafts were an inherent error in the updraft calculations, we would see a strong Gaussian white noise fluctuation with radius and azimuth
- Rather, we see that radial occurrences decrease outside of the inner core and we see strong peaks azimuthally in the downshear quadrants with convective suppression in the USL quadrant